

## High-Frequency Radiation from an Earthquake Fault: A Review and a Hypothesis of Fractal Rupture Front Geometry

A. A. GUSEV<sup>1,2</sup>

**Abstract**—Observed high-frequency (HF) radiation from earthquake faults exhibits specific properties that cannot be deduced or extrapolated from low-frequency fault behavior. In particular: (1) HF time functions look like random signals, with smooth mean spectrum and moderately heavy-tailed probability distribution function for amplitudes; (2) well-known directivity of low-frequency radiation related to rupture propagation is strongly reduced at HF, suggesting incoherent (delta-correlated) behavior of the HF radiator, and contradicting the usual picture of a rupture front as a regular, non-fractal moving line; (3) in the spectral domain, HF radiation occupies a certain specific band seen as a plateau on acceleration source spectra  $K(f) = f^2 M_0(f)$ . The lower cutoff frequency  $f_b$  of  $K(f)$  spectra is often located significantly higher than the common spectral corner frequency  $f_c$ , or  $f_a$ . In many cases, empirical  $f_b(M_0)$  trends are significantly slower as compared to the simple  $f_b \propto M_0^{-1/3}$ , testifying the lack of similarity in spectral shapes; (4) evidence is accumulating in support of the reality of the upper cutoff frequency of  $K(f)$ : fault-controlled  $f_{max}$ , or  $f_{uf}$ . However, its identification is often hampered by such problems as: (a) strong interference between  $f_{uf}$  and site-controlled  $f_{max}$ ; (b) possible location of  $f_{uf}$  above the observable spectral range; and (c) substantial deviations of individual source spectra from the ideal spectral shape; (5) intrinsic structure of random-like HF radiation has been shown to bear significant self-similar (fractal) features. A HF signal can be represented as a product of a random HF “carrier signal” with constant mean square amplitude, and a positive modulation function, again random, that represents a signal envelope. It is this modulation function that shows approximately fractal behavior. This kind of behavior was revealed over a broad range of time scales, from 1 to 300 s from teleseismic data and from 0.04 to 30 s from near-fault accelerogram data. To explain in a qualitative way many of these features, it is proposed that rupture propagation can be visualized as occurring, simultaneously, at two different space–time scales. At a macro-scale (i.e. at a low resolution view), one can safely believe in the reality of a singly connected rupture with a front as a smooth line, like a crack tip, that propagates in a locally unilateral way. At a micro-scale, the rupture front is tortuous and disjoint, and can be visualized as a multiply connected fractal “line” or polyline. It propagates,

locally, in random directions, and is governed by stochastic regularities, including fractal time structure. The two scales and styles are separated by a certain characteristic time, of the order of  $(0.07–0.15) \times$  rupture duration. The domain of fractal behavior spans a certain HF frequency range; its boundaries, related to the lower and upper fractal limits, are believed to be manifested as  $f_b$  and  $f_{uf}$ .

**Key words:** High-frequency radiation, earthquake source, rupture, upper cutoff frequency, source acceleration spectrum, fractal.

### 1. Introduction

The last 30 years witnessed great progress in analysis, modeling and inversion of earthquake fault processes. Still, the emphasis of this progress was on signals that constitute the lower-frequency part of earthquake source spectrum. Generally, the fault process is rather broad-band, and for the largest events fills the entire observable range of 0.003–30 Hz covered jointly by teleseismic and near-fault observations. Thus, it may be useful to analyze low-frequency (LF) and high-frequency (HF) sub-ranges separately. Traditionally, as HF or short-period energy, one understands a signal component in the frequency range above 0.3–0.5 Hz, best recorded by a teleseismic short-period instrument or strong-motion accelerograph. This definition is adequate in terms of required observational systems, or from the earthquake-engineering viewpoint. Still, it is less adequate when one seeks to understand the fault behavior. From this viewpoint, when analyzing a particular earthquake, it might be more appropriate to separate the related frequency range into LF and HF parts on the basis of intrinsic temporal parameter, that of fault corner frequency  $f_c \approx 1/T_c$  where  $T_c$  is the source process duration. The boundary frequency separating LF and

<sup>1</sup> Institute of Volcanology and Seismology, Russian Academy of Sciences, Petropavlovsk-Kamchatsky, Russia. E-mail: gusev@emsd.ru

<sup>2</sup> Kamchatka Branch, Geophysical Service, Russian Academy of Sciences, Petropavlovsk-Kamchatsky, Russia.

HF ranges can be selected about  $5\text{--}8 f_c$ . To underline the difference between these cases we shall sometimes refer to them as relatively high frequency (RHF) and relatively low frequency (RLF), preserving the denotations HF and LF for the traditional usage. Each of the two definitions may be preferable in different situations. These two modes of division of the complete frequency range into two parts approximately coincide with the magnitude range 6–7. In our revised definition, when mentioning RHF, we always speak about wavelengths much shorter than fault length, and one can expect this part of fault radiation to have specific properties.

The aim of the present paper is twofold: to shortly review the specific properties of HF (RHF) radiation, and on this basis to derive some concepts regarding properties of rupture that may underpin the presented observations. The following list of properties of HF (RHF) radiation is proposed as its main and specific features:

- random-like (noise-like) appearance of signals; smooth mean spectra;
- specific spectral shape with a plateau in the source acceleration spectrum (“ $\omega$ -square behavior”) bounded by two specific cutoff frequencies: by the lower cutoff  $f_b$  on the LF side; and, in many cases, by the upper cutoff, i.e. fault-controlled  $f_{\max}$ , in the range from 3 to 30 Hz and above, on the HF side;
- deteriorated or absent directivity of RHF radiation;
- non-Gaussian, moderately heavy-tailed probability distribution of amplitudes;
- random self-similar (fractal) organization of envelopes of radiated RHF body waves;
- lack of coincidence between high-slip and high-HF-radiation spots over the fault area.

The last point was covered in the recent review by NAKAHARA (2008), see also GUSEV *et al.* (2006); it was shortly discussed elsewhere (GUSEV 2011). Thus, it was decided not to include this interesting but somewhat detached point into the current review.

If one compares the listed observed properties to the picture that can be expected for a standard reference rupture model of propagating shear crack, one notes several lines of expressed disagreement. This disagreement can be analyzed to improve the understanding of fault processes.

As a particular step in this direction, a general concept of band-limited fractal rupture front is proposed based on the joint analysis of the listed properties. The upper frequency bound of the fractal behavior is associated with fault-controlled  $f_{\max}$ . The lower-frequency bound may be associated with one or more of the following three characteristic critical frequencies: (1) the boundary frequency between domains of weak HF (RHF) directivity and clear LF (RLF) forward directivity; (2) the LF (RLF) cutoff of the acceleration spectral plateau  $f_b$  and (3)  $1/T_{\text{rise}}$ , where  $T_{\text{rise}}$  is the duration of local slippage (slip pulse) at a point of a fault.

## 2. Random, Noise-Like Appearance of Time Functions; Smoothness of Mean Spectra

The specific appearance of HF time functions radiated by an earthquake source is best illustrated by recorded body waves. There are two cases when HF waves dominate on a record, with limited distortion related to propagation. First it is the case when direct HF S-waves constitute a maximum-amplitude part of a near-fault accelerogram (still, not too close to the fault; otherwise a static/non-wave term contribution may be prominent, making such records less convenient for analysis). Secondly, it is the case of teleseismic *P*-wave trace, specifically from events with magnitude about 7 or larger, when path-related effects of scattering become secondary. These signals typically look like modulated random noise, with their duration defined, mostly and on average, by the source process duration. However, the observed duration is affected also by rupture propagation effects, with compression to forward and expansion in backward direction. This effect operates in addition to along-path propagation effects proper, that always increase duration at a receiver as compared to duration at the source. The durations of the signal mostly match well for HF and LF signals; thus, one can believe that they are generated by the same rupture process. Still, within this common time window, their amplitudes are, generally, far from being well correlated. This lack of close correlation reflects the mismatch of LF- and HF-signal generation areas along the fault, as was mentioned above.

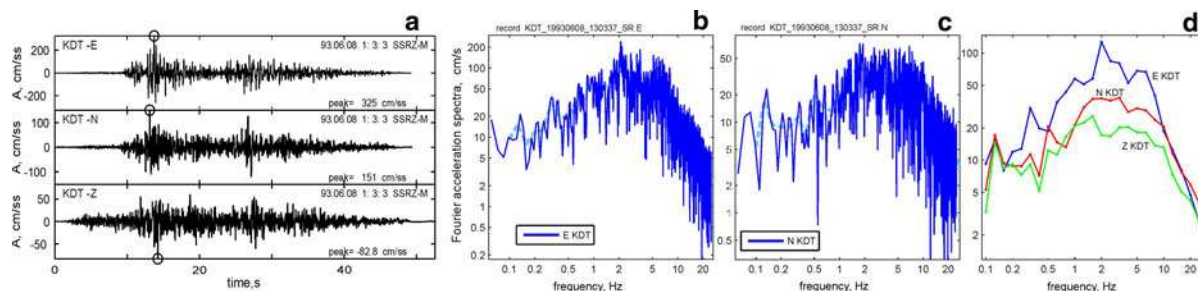


Figure 1

High-frequency (acceleration) time functions of 1993.06.08,  $M_w 7.5$ ,  $H = 40$  km, Kamchatka earthquake as recorded by station KDT at the epicentral distance 70 km. **a** Three components of ground motion; **b**, **c** amplitude spectra of horizontal traces of **a**; **d** smoothed amplitude spectra of three components, smoothing window width 0.1 log10 units (1/3 octave)

On Fig. 1a a typical random-looking accelerogram is shown, with dominating S-wave HF signal on three components, and with a preceding P-wave HF signal (well seen on vertical component;  $P$  arrival lost) whose later part drowns in much more energetic S-wave train. As usual with random-like signals, finding spectra is a powerful instrument for their analysis. Fig. 1b, c represent Fourier amplitude spectra of horizontals. The general appearance includes approximately flat maximum central part, which is predicted by the common  $\omega^{-2}$  model for source spectra. The upper cutoff and further roll-off is related to the frequency-dependent path attenuation, with the primary role of “site-controlled  $f_{\max}$ ” effects related to high attenuation immediately under the station. Low-frequency cutoff is also seen. At first glance it can be associated with the standard corner frequency  $f_c$ . Its actual origin must be different however because the position of this cutoff, around 0.5–1 Hz, clearly disagree with the usual  $f_c$  estimate  $f_c \approx 1/T_c$ , where the apparent rupture duration time  $T_c$  must be around 35 s as well seen from the duration of the dominating S-wave group on Fig. 1a. This estimate matches well the teleseismic body-wave estimate of 30 s following JOHNSON *et al.* (1995). Therefore, the observed LF cutoff of acceleration spectrum located at 0.5–1 Hz cannot represent the classical corner frequency  $f_c$  of the Aki-Brune spectral model. Rather, this cutoff is an example of a specific feature of the spectral shape with two corners or two humps (GUSEV, 1983; IZUTANI, 1984; PAPA-GEORGIOU and AKI, 1985). This feature will be denoted  $f_b$  following ATKINSON (1993). Between cutoffs, the unsmoothed amplitude spectrum is noisy but shows

no significant features; its absolute level is stable. A peak seen on one of the spectra can be considered an insignificant peculiarity, or, in terms of a stochastic view on the spectrum, a fluctuation.

The appearance of the observed amplitude spectrum like the one seen in Fig. 1b, c evidently invites smoothing that might reveal spectral trends in more stable manner. However, despite the fact that smoothing is rather useful in practice, its application lacks generally accepted theoretical foundation, and its use may raise questions regarding formal meaning of this operation as well as its lawfulness. This important point deserves special discussion, planned for presentation elsewhere. Speaking briefly, one should, following HASKELL (1964, 1966) introduce a mean (ideal, ensemble-average) energy spectral density function (at a source), and corresponding mean signal energy spectrum at a receiver. In earthquake data analysis, one seeks to derive an empirical estimate of signal energy spectrum from short segments of fluctuating, random-noise-looking data. To do this one can liken energy spectral density to power spectrum integrated along time, and based on this analogy, develop the smoothing procedure as averaging of the observed squared Fourier amplitude spectrum over an appropriate spectral window. Then the square root of the averaged square spectrum can be calculated, resulting in the sought for smoothed amplitude spectrum, that can be viewed as an appropriate statistical estimate for the ideal one.

The use of a particular spectral window or windows is not dictated by such a theory. The tradition of power spectrum estimation and some work in seismology suggests using a constant-width smoothing

window. However, when one is interested in spectral trends represented by power laws, as is typically the case in earthquake seismology, more appropriate is the use of logarithmically-uniform spectral points and corresponding logarithmically-uniform window widths. The price for this is variable statistical accuracy that deteriorates at the low-frequency side of the spectrum. At this side, the smoothing operation cannot be performed at frequencies below  $2\text{--}5 f_c$ ; because for this operation to be meaningful, one needs a few independent points of Fourier spectrum within a smoothing window. Therefore, over the range  $(1\text{--}5) f_c$ , one must confine the analysis by deterministic approach. In particular, it is near to impossible to determine accurately the spectral trend or slope within this range. Another problem with spectral smoothing can and does arise at parts of the spectrum with fast variation, especially with the steep roll-off at the HF side, as is the case for the example spectrum of Fig. 1. To obtain a more accurate estimate in such a case, the well-known prewhitening filter can be designed and applied before smoothing; the results of smoothing are then “colored back”. One more possible improvement is the use of multi-taper procedure.

With a deeper theory absent, the selection of a particular value for logarithmic bandwidth is somewhat subjective; often, the useful range is between  $1/3$  and  $1$  octave (ten to about three points per decade) making moderate or strong smoothing. In Fig. 1d we show the result of moderate ( $1/3$  octave) spectral smoothing. No visually remarkable spectral peaks can be seen in unsmoothed spectra that might be suppressed by smoothing. This behavior is quite typical; it can be seen as an indication that mean (ensemble-average) radiated and observed spectra are, essentially, slow varying functions of frequency, and in particular that a rupture, typically, does not generate non-trivial sinusoids. Note that for a smoothing operation to be correct, one must make a prior assumption that “ideal” spectrum is a slow varying function. This kind of circularity is inevitable in practical data processing that is always based on some prior assumptions.

Not all dynamic friction phenomena produce so dull a signal, as an example of a violin shows; thus, the noise-like appearance of a HF signal is not

absolutely trivial. This fact can be considered an indication of random space–time organization of fault rupturing history. Noise-like components of the signal can be seen simultaneously over many frequency bands and reveal the multiplicity of scales of the rupture process over space and time. Within a particular scale/band, random signal amplitudes will be shown later to behave in a specific, systematic way, resulting in self-similar or fractal temporal structure of a corresponding envelope.

### 3. Deteriorated or Absent Directivity of HF Energy

An important property of HF earthquake radiation is its low or lacking directivity effect. This phenomenon is complicated and comprises features of two different kinds. First, there are effects (or the lack of) related to the point-source radiation pattern. The second kind is the lack of directivity narrow sense, related to a particular, typically unilateral manner of the propagation of a rupture. These two phenomena can and do combine, making their separation a complicated task. This task is aggravated by the coincidence of critical frequency bands: both kinds of directivity manifest themselves clearly below the  $0.5\text{--}2$  Hz range and disappear at frequencies above it. Despite these problems, at present a relatively clear picture can be outlined.

For an extended source of a large magnitude earthquake it is not easy to observe the radiation pattern at HF. The isotropization of the radiation pattern of the near-source HF signal was accurately established by LIU and HELMBERGER (1985) for near-fault records of a moderate event, with complex non-planar faulting as a preliminary explanation. YU *et al.* (1995) noted effects of isotropization of the radiation pattern and assumed that both scattering along a ray path and local perturbations of fault rake angle make contributions to this phenomenon. Later work (SATO, 2002; TAKENAKA *et al.*, 2003; CASTRO R *et al.* 2006; TAKEMURA *et al.*, 2009) has shown that effects of scattering alone seem to be sufficient. The observed behavior for both frequency dependence and distance dependence of the “smearing” of the theoretical radiation pattern has been successfully simulated on this basis. The discussed phenomenon is characteristic of a point

source, and best studied with data from small to moderate events. For large earthquakes at local to regional distances, smearing effects of scattering on a point-source radiation pattern mix with blurring effects of the finite-size radiator; thus, the two effects may be difficult to isolate accurately.

Consider now effects of directivity narrow sense, related to the properties of space–time history of propagating rupture. In the simplest case of a narrow unilateral rupture, directivity effects (aka Doppler effects) are well known and reduce to compression of a forward-radiated pulse and expansion of a backward-radiated one. The classic theory of BEN-MENACHEM, (1961, 1962) (originally formulated in the frequency domain) for unilateral line source of length  $L$  rupturing at a constant velocity  $v_{\text{rup}}$  predicts far-field time function for body waves displacement in homogeneous medium as a boxcar pulse with duration  $T$  and amplitude  $A$ :

$$T = T(\theta) = L/v_{\text{rup}}D(\theta) \quad (1)$$

$$A = A(\theta) = CM_0/T(\theta) = C'M_0D(\theta) \quad (2)$$

where  $D(\theta)$  is the directivity factor

$$D(\theta) = 1 / \left( 1 - \left( \frac{v_{\text{rup}}}{c} \right) \cos \theta \right) \quad (3)$$

$M_0$  is seismic moment,  $\theta$  is the angle from the forward direction to the ray to a receiver,  $c$  is wave velocity, and  $C$ ,  $C'$  as well as  $C''$ ,  $C'''$  below are constants irrelevant for the present discussion. It is difficult to analyze directivity effects on velocity amplitudes, as velocity time history is singular for this simple model. Modifying this model for more realism BOORE and JOYNER (1978) assumed that slip amplitude depends on the position on the fault. In the simpler of their models, one with constant  $v_{\text{rup}}$ , time function of the displacement signal at the receiver is expanded or compressed along time axis in accordance with  $T(\theta)$  or  $1/D(\theta)$ . The area of displacement pulse is  $CM_0 = \text{const}$  at any  $\theta$ , whereas signal amplitude is controlled again by the  $D(\theta)$  factor. However, different from the case of a boxcar pulse, we can now lawfully pass to velocity signal and obtain for its (rms) amplitude  $A_v$ .

$$A_v(\theta) = C''M_0/T^2(\theta) = C'''M_0D^2(\theta) \quad (4)$$

As signal energy  $E$  is proportional to  $A_v^2T$ , one readily obtains

$$E(\theta) \propto M_0^2D^3(\theta) \quad (5)$$

As for corresponding Fourier amplitude spectrum, it also has a fixed (normalized) shape, and it is squeezed or stretched along frequency axis in proportion to corner frequency  $f_c \propto 1/T(\theta)$ . This is true also for mean square velocity spectrum; thus, rms HF spectral levels are strongly dependent on  $\theta$ . For a certain fixed frequency band  $\Delta f$  around  $f$ , for the case of  $\omega^{-\gamma}$  displacement spectral shape at HF, rms level of amplitude spectrum for velocity signal behaves as

$$V_f(f) = E^{0.5}(f, \Delta f) \propto M_0T(\theta)^{-\gamma} \propto M_0D(\theta)^\gamma \quad (6)$$

(with typically  $\gamma = 2$ ). To summarize, directivity effects can be expected to be equally prominent at low and high frequency. This line of reasoning was further developed by JOYNER (1991) and HERRERO and BERNARD (1994). It was gradually realized, however, that for the observed spectra, their HF part does not follow this theoretical implication: recorded HF amplitudes and spectral levels seem to be almost independent on azimuth, and there is no strong forward enhancement of HF amplitudes (TSAL, 1997, SOMERVILLE, 1997; GALLOVIC and BURJANEK, 2007).

A comment on terminology is relevant here. Random-slip models of the described kind, considered by BOORE and JOYNER (1978), JOYNER (1991) and HERRERO and BERNARD (1994) are sometimes called “incoherent”. This usage looks disputable. The reference “coherent” case appears when rupture propagates with well-defined, smoothly changing velocity, and there are deterministic phase relationships between contributions of various spots of the fault to the signal at a receiver. This phase-stability property results, in particular, just in the expressed forward enhancement of amplitudes. This reasoning is valid equally well both for deterministic and random amplitudes: in both cases, phase/time delays at the receiver are deterministic and signal contributions add up coherently. Therefore, truly incoherent behavior can be reduced neither to generation of a rugged signal shape, nor to arbitrary randomization of the fault behavior (e.g. by perturbing local slip rate, or local rupture velocity); it must include randomization of phases. In its simplest form the property of incoherence requires source function to be uncorrelated in space–time. For a multitude of small spots covering the fault area, consider

their HF contribution into the receiver amplitude for a certain frequency band  $\Delta f$  around  $f$  [the size of a spot defines the coherence radius; see GUSEV (1983) for more details]. For such a source, each of these contributions is an independent random value with zero mean and a certain value of mean square. In the summation of random summands, mean squares are additive. Thus, we come to the additivity of mean square amplitudes, which is the main property of the incoherent source. The considered sum of contributions at the receiver is the joint square amplitude, with definite mean (instant power, further called envelope). To relate this model with more traditional seismological models of a rupture one may assume that individual rupture spots are triggered in such a way that their onset time versus distance relationship does not form a monotonous sequence. The crucial role of non-monotonous temporal structure was already mentioned by BOORE and JOYNER (1978); recently it was underlined by DAY *et al.* (2008) who note that to create deterioration of directivity at high frequencies, one should “model rupture complexity in a form that permits rupture to be omnidirectional at small length scales, even though unidirectional at large scales,” whereas simple modulation of the magnitude of slip rate over a fault cannot effectively suppress enhanced forward directivity. It should be mentioned that such behavior is quite permissible from the elastodynamic viewpoint: dynamic simulations with sufficiently inhomogeneous stress drop or strength support the possibility of disjoint/fragmented ruptures that are needed to form incoherence of a HF source (DAY, 1982; BOATWRIGHT and QUIN, 1986; SPUDICH and OPPENHEIMER, 1986).

There are many models that in essence assume incoherent behavior of earthquake source; however, in most of them this property is not formulated explicitly [the first explicit reference to incoherency of the source is probably KOSTROV (1974)]. This line of study included primitive random multiple-subevent source models of BLANDFORD (1975) or HANKS (1979) who abstracted themselves from the finiteness or temporal organization of the source. Models of finite-fault HF radiation with independently radiating fault patches or with randomly phased subsources whose onset times are random were then proposed by PAPAGEORGIOU and AKI (1983, 1985); GUSEV (1983, 1989); KOYAMA

(1985); ZENG *et al.* (1994); ROGERS and PERKINS (1996). In addition to random time delay, KOYAMA (1985) hypothesized a locally random propagation direction, uncorrelated between adjacent patches.

A significant conceptual and practical issue is one of the spatial structure of incoherent radiation field around a finite earthquake fault. A distribution of HF amplitudes in space near to an incoherent source was analyzed by GUSEV (1983) for a radiating disk source. TRIFUNAC and LEE (1989) successively applied this theory to empirical data on acceleration spectra observed in the vicinity of rupturing faults, providing an effective check of the incoherence hypothesis. For one more check of this kind see OHNO *et al.* (1993). Along similar lines, PAPAGEORGIOU and AKI (1985) derived a formula for another source geometry, that of radiating strip; and SINGH *et al.* (1989) and OHNO *et al.* (1993) refined Gusev's results for disk introducing more realistic amplitude decay for a point source ( $e^{-\alpha r}/r$  instead of simple  $1/r$ ). Later GUSEV and SHUMILINA (2000) developed a numerical approach to the problem, with finite source represented as a rectangular grid of subsources, and more general, empirically-based attenuation function of a point source. A significant notion of fault coherence radius, assumedly frequency-dependent, was introduced by GUSEV (1983) who mentioned that “total” incoherency, with delta-correlated radiating surface, must lose adequacy very near to a fault.

As for the temporal structure of HF radiation from an incoherent source, the results discussed above with respect to displacement pulse amplitudes from line sources can be easily modified with respect to squared amplitudes or envelopes of random signals, see e.g. (GUSEV and PAVLOV 1991). Let  $P(t, f, \Delta f | \theta)$  be mean square amplitude (record envelope) at a distant receiver in a HF band  $\Delta f$  around  $f$ . Integrating  $P(\cdot)$  over time one obtains total energy  $E(f, \Delta f)$

$$E(f, \Delta f) = \int_0^{T(\theta)} P(t, f, \Delta f | \theta) dt \quad (7)$$

where the dependence of  $E(f, \Delta f)$  on  $\theta$  disappears, in complete analogy with the area of LF body wave displacement pulse that defines  $M_0$  simultaneously for any  $\theta$ . Then for time-averaged envelope  $\bar{P}(t, f, \Delta f | \theta) = \bar{P}(f, \Delta f | \theta)$  and for time-averaged rms

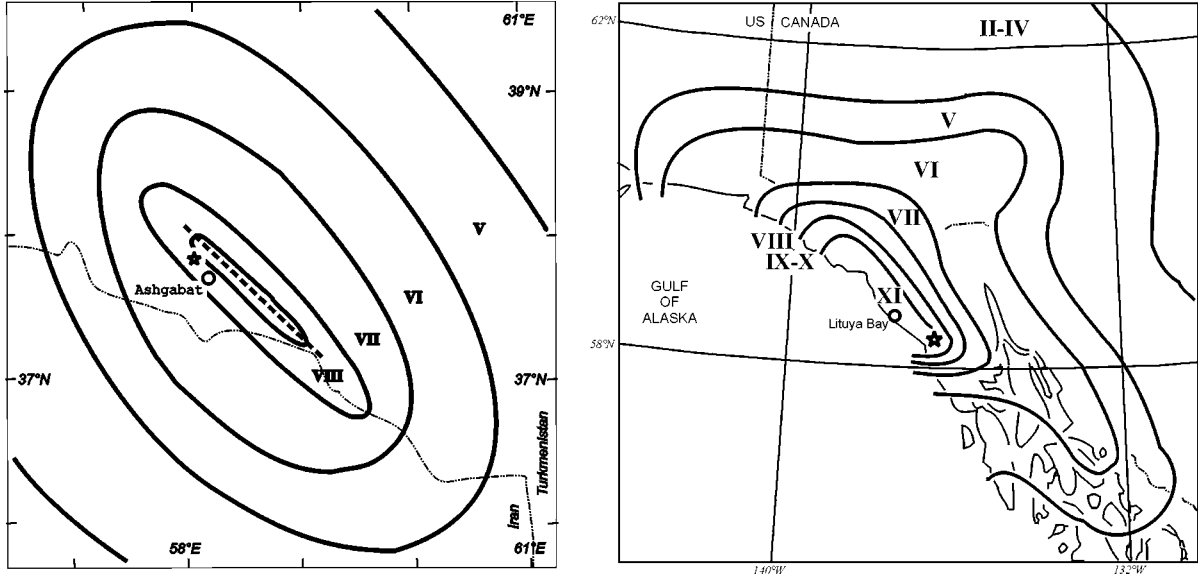


Figure 2

Isoseismal maps of two large earthquakes with unilateral rupture showing no directivity. Roman numerals are intensity grades, MM or MSK scale, epicenters are marked by stars. *Left*: 1948.10.05, M7.3 Ashgabat, Turkmenistan, earthquake, modified from (SHEBALIN 1974). *Right*: 1958.07.10, M7.8 Lituya Bay, Alaska earthquake, modified from (Stover and Coffman 1993)

amplitude  $\overline{a_{rms}}(f, \Delta f | \theta) = \overline{P}^{0.5}(f, \Delta f | \theta)$  at the receiver one can write

$$\overline{P}(f, \Delta f | \theta) \propto E(f, \Delta f) / T(\theta) \propto E(f, \Delta f) D(\theta) \quad (8)$$

$$\begin{aligned} \overline{a_{rms}}(f, \Delta f | \theta) &\propto E^{0.5}(f, \Delta f) / T^{0.5}(\theta) \\ &\propto E^{0.5}(f, \Delta f) D^{0.5}(\theta) \end{aligned} \quad (9)$$

Here  $\overline{a_{rms}}(f, \Delta f | \theta)$  describes time-domain amplitudes of acceleration signal with central frequency  $f$  and bandwidth  $\Delta f$ . Therefore, in a limited analogy with displacement pulses in the deterministic case, mean square amplitude of a pulse (9) is dependent on direction, but directivity enhancement for HF amplitudes is much weaker as compared to LF amplitudes, as it is proportional to  $T^{-0.5}$ , not  $T^{-1}$ . Amplitude directivity of this kind is often difficult to notice. To obtain estimates for frequency domain, one can divide  $E(f, \Delta f)$  by  $\Delta f$  and take square root to obtain the estimate of rms amplitude spectrum

$$a_{f,rms}(f) = (2E(f, \Delta f) / \Delta f)^{0.5} \quad (10)$$

Thus, for the case of incoherent source, Fourier amplitude spectral level shows no directivity at all (again analogous to LF spectral level of displacement spectrum). For the important case of response spectrum, the expected behavior is the intermediate one

between the cases of time-domain and Fourier-spectral amplitudes. Thus, weak directivity may be expected at RHF. The entire discussion above is for the far field of a finite source, whereas in the vicinity of a fault, the picture is more complicated. Still, the general tendency can be expected to be the same.

Data analysis in many cases shows that real earthquake sources generate HF signals whose directivity properties agree with the idea of an incoherent source. Figure 2 shows isoseismal maps for two large earthquakes with clearly unilateral rupture propagation. In both cases, that are quite typical, directivity imprint is unobservable for macroseismic intensity that is defined mostly by HF signal. Still, in some cases, the presence of moderate directivity imprint was noted for intensity data (KOYAMA and IZUTANI 1990).

Directivity for response spectral amplitudes was studied in detail by SOMERVILLE (1997) and ROWSHANDEL (2006, 2010). In Fig. 3 from (ROWSHANDEL 2006) one can clearly see expressed directivity below 0.7 Hz (period >1.5 s), and low but still existent directivity above 1 Hz (period <1 s).

The qualitative result regarding weak directivity of response spectral amplitudes for frequency bands 1–5 Hz can be reliably extended to the similar behavior of peak acceleration. For peak velocities,

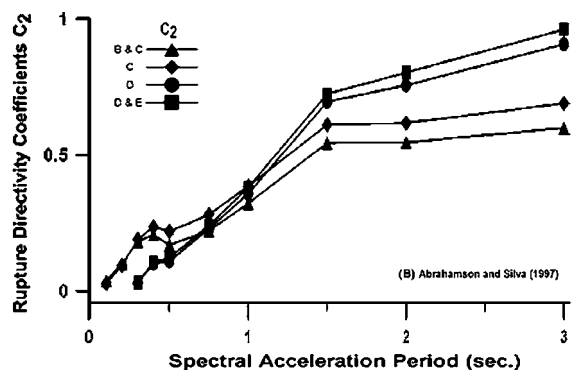


Figure 3

Coefficient  $C_2$  of the slope of  $\log$  (response spectral acceleration) versus “effective directivity  $x_i$ ” parameter, where  $x_i$  is a weighted average of  $\cos\theta$  for a given receiver. Separate lines are plotted for subsets of data with different soil conditions at a recording site. Modified from Fig. 4 of (ROWSHANDEL 2006)

the situation is different because their typical characteristic frequencies, of 0.3–1.5 Hz, correspond to the boundary zone between the two kinds of behavior; in fact, clear directivity features can be expected and are actually observed for the velocity signal (SOMERVILLE *et al.*, 1997; SOMERVILLE, 1998; MAVROEDIS and PAPAGEORGIOU, 2003).

The transitional frequency between ranges of high and low directivity shall be denoted  $f_{ucoh}$ , for the “upper bound of coherent behavior.” The observed range  $f_{ucoh} = 0.7\text{--}1.5$  Hz has not been directly associated with earthquake magnitude or rupture duration. However, it should be mentioned here that directivity effects in many cases are also clearly observed for small-to-moderate earthquakes, for peak velocities and accelerations, sometimes even at 10 Hz (BAKUN *et al.*, 1978; BOATWRIGHT, 2007; SEEKINS and BOATWRIGHT, 2010). In the present context, these facts suggest that  $f_{ucoh}$  follows corner frequency and shifts up with respect to its value for  $M = 6\text{--}7$  earthquakes studied by SOMERVILLE *et al.* (1997). In other words, acceleration signal from smaller earthquakes is, rather, “relative-LF” signal, and thus can and must show directivity. Oppositely, ABRAHAMSON (2000) and ROWSHANDEL (2010) note weaker directivity effects at smaller magnitudes ( $M < 6$ ); these results disagree with the present viewpoint. More studies are evidently needed.

To specify  $f_{ucoh}$  relation to magnitude is difficult; the more so because some events show trends

opposite to the general tendency (ROWSHANDEL 2010). ROWSHANDEL (2010) do not mention any magnitude dependence of the boundary period for directivity, and such a dependence, even if real, probably cannot be resolved from scarce and noisy collected data that mostly cover the limited magnitude range 6.5–7.5. Assuming the transitional period range  $1/f_{ucoh} = 1\text{--}2$  s, the ratio  $T_c(M = 7)/T_{ucoh} \approx 16/1.5 \text{ s} \approx 10$ . Below  $f_{ucoh}$ , both far-field and specifically near-field signals become coherent, in particular in the forward direction, and form a “forward-directivity pulse” (SOMERVILLE *et al.*, (1997); SOMERVILLE 1998, 2003) that has attracted much attention in earthquake engineering. Duration and/or period of such a pulse,  $T_{dir}$ , can be probably considered as a lower bound for  $1/f_{ucoh}$ . This parameter show clear increase with magnitude, with a typical value of  $T_c/(4\text{--}5)$ .

#### 4. Fourier Spectral Shapes at High Frequency.

##### Lower Source Acceleration Spectral Cutoff $f_b$

Source (displacement) spectrum in the relative-HF range is fast decaying. The source acceleration spectrum forms a plateau (Fig. 4). This plateau is reflected as similar behavior of Fourier spectra of

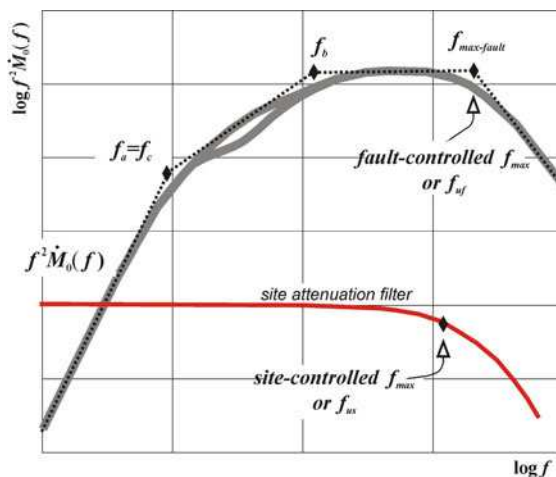


Figure 4

A sketch of the shape of source acceleration spectrum  $K(f) = f^2 M_0(f)$  of a moderate-to-large earthquake. The standard single-corner  $\omega^{-2}$  model corresponds to the case  $f_b = f_a = f_c$  and  $f_{uf} = \infty$ . The spectral trend between  $f_a$  and  $f_b$  is shown in two variants. The lower curve depicts site-attenuation filter that produces site-controlled  $f_{max}$  or  $f_{us}$

observed near-fault ground motions, with certain distortions related to path and site-geology effects. The acceleration spectral plateau corresponds to the  $\omega^{-2}$  HF decay of displacement source spectrum. Such spectra were proposed in the stochastic model of AKI (1967) and in the deterministic model of BRUNE (1970). Actually, BRUNE (1970) proposed more general spectral model, of  $\omega^0-\omega^{-1}-\omega^{-2}$  kind, with two corners separated by an intermediate slope, but this idea was not developed in the 1970s. Later it was found that deterministic flat acceleration amplitude spectra of the Brune's model can be treated as a stochastic phenomenon. This approach happened to be rather efficient for the description of properties, and further for simulation, of observed accelerograms (HANKS and MCGUIRE, 1981; BOORE, 1983, 2003). The accelerograms are treated, for this aim, as segments of band-limited white noise. An important property of AKI (1967) and BRUNE (1970) source spectral models is similarity of source spectra for various magnitudes (or  $M_0$ ). Similarity of real source spectra was put under doubt by AKI (1972), then GUSEV (1983) proposed empirically-based spectral scaling law lacking similarity, with three characteristic frequencies that are not proportional to one another.

Following (ATKINSON, 1993), here we shall call the two lower among them as  $f_a$  and  $f_b$  (other denotations for  $f_b$  are  $f_c^*$ ,  $f_2$  and  $f_{c2}$ ). The uppermost corner, "fault-related  $f_{\max}$ ", here denoted  $f_{\text{uf}}$ , is discussed in detail in the next section. The lowermost one,  $f_a$ , is close to the common corner frequency  $f_c$ , and is defined mostly by rupture duration  $T_c \approx 1/f_a$ . Directivity effect on  $f_a$  may be significant, but irrelevant here, and we shall consider  $f_a$  as an average over focal sphere. Sometimes  $f_c$  is defined as  $(f_a f_b)^{0.5}$  (as the intersection of  $\omega^{-0}$  and  $\omega^{-2}$  asymptotes) and in such a case it is not identical to  $f_a$  (that represents the intersection of  $\omega^{-0}$  and  $\omega^{-\gamma}$  with adjustable higher-frequency asymptote with  $\gamma = 0.5-2$ ). In accordance with common scaling of earthquake ruptures (KANAMORI and ANDERSON, 1975),  $1/T_c \approx f_a \propto M_0^{-1/3}$ . As for  $f_b$  (GUSEV, 1983; IZUTANI, 1984; PAPAGEORGIOU and AKI, 1985; PAPAGEORGIOU, 1988), its value is typically in the range  $2-10f_a$ . Not infrequently, the spectral shape between  $f_a$  and  $f_b$  happens to be concave, forming, in displacement or velocity spectrum, a spectral hump around  $f_b$ . Still, less prominent behavior, simply with two corners, is more common

(c.f. BOATWRIGHT and CHOY, 1989, 1992). In a certain fraction of cases, the  $f_b$  corner is not observed resulting in a simple  $\omega^{-2}$  shape, and this is more often the case for lower-magnitude earthquakes.

Such cases do not definitively undermine the concept of  $f_b$  as a standard feature of source spectrum. It can be unobservable for one of a few causes: (1) when the assumed path attenuation correction is too low (as often the case for the analysis of teleseismic data), pressing down the  $f_b$ -related corner; (2) when shorter-period surface waves enhance the observed record energy in the 0.1–1 Hz range, above  $f_b$ , whereas in the data analysis, the  $1/r$  geometrical spreading is assumed; (3) when acceleration spectral plateau is positioned low for natural reasons, and its low frequency edge, or  $f_b$ , is impossible to detect reliably; and at last (4) when statistical scatter precludes any reliable determination of  $f_b$ . Even when the intermediate spectral slope between  $f_b$  and  $f_a$  is discernible, it may systematically deviate from unity (BOATWRIGHT and CHOY, 1989).

Situation is additionally complicated by the widespread prior assumption that one-corner BRUNE (1970) model must be true. When this assumption is taken as the basis of data analysis, the intermediate spectral segment with approximately  $\omega^{-1}$  behavior is often ignored or lost. As a result, no  $f_b$  estimate is constructed, the estimated  $f_c = f_a$  is an intermediate value between the true  $f_a$  and true  $f_b$ , and the stress drop is overestimated. It deserves reminding that when THATCHER and HANKS (1973) analyzed many local earthquake spectra with no prior assumption of a single " $\omega^0-\omega^{-2}$ " corner, they obtained stress drop values significantly lower than usual, often associated with approximately  $\omega^{-1}$  spectral HF behavior just above the corner. In 1980–2000 many studies of spectral scaling established the reality of the  $f_b$  feature (e.g. for western USA: TRIFUNAC (1993), ATKINSON (1997); for ENA: ATKINSON (1993); see Fig. 5 for these and more trends). Nowadays  $f_b$  is a standard feature of most average Fourier spectrum scalings, either implicitly or explicitly.

An important but controversial property of  $f_b$  is the mode of its decrease with increased magnitude. In the 1980s, most researchers believed that  $f_b$  decreases with  $M_0$  slower as compared to the common corner  $f_a$ . Because of this behavior, there exists a general tendency of  $f_a$  and  $f_b$  to merge at small magnitudes.

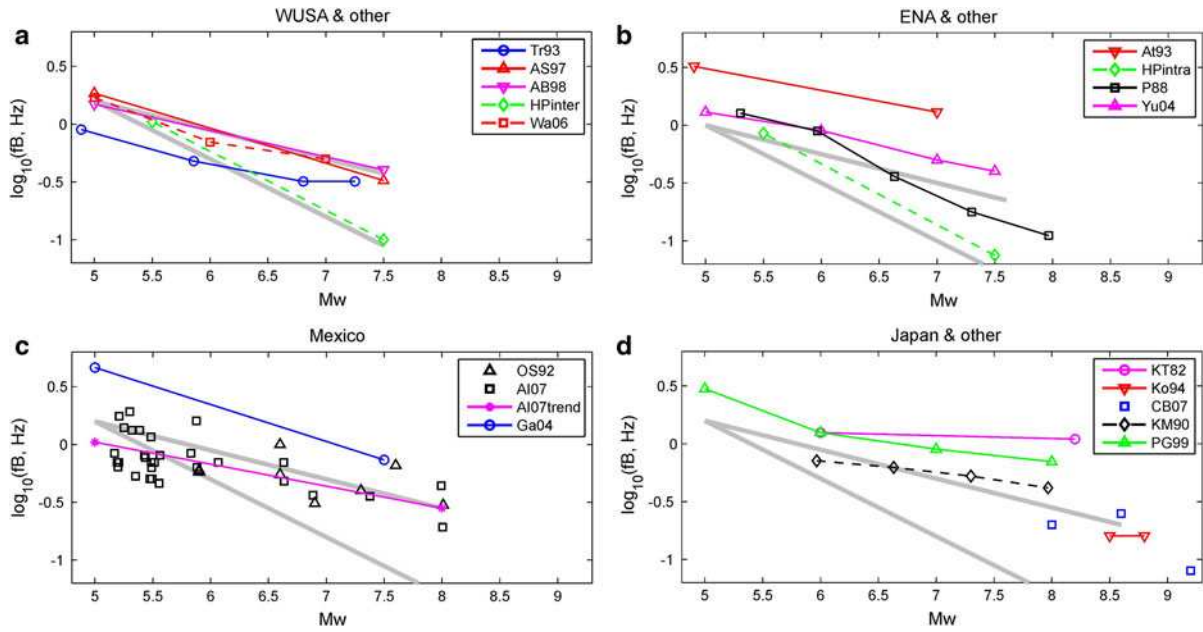


Figure 5

Compilation of empirical trends of the second corner frequency,  $f_b$ , of source spectra, versus  $M_w$ . **a** Western North America: Tr93: (TRIFUNAC 1993); AS97: (ATKINSON 1997); AB98: (ATKINSON and BOORE 1998); HPinter: (HALLDORSSON and PAPAGEORGIOU 2005, interplate data subset); Wa06: (WANG *et al.* 2006). **b** At92: Eastern North America—higher stress drop territory (ATKINSON 1993); HPintra: intraplate data subset after (HALLDORSSON and PAPAGEORGIOU 2005); P88: general trend according (PAPAGEORGIOU 1988); Yu04: former Yugoslavia after MANIC (2004). **c** Mexico shallow depth: OS92: data points derived from plots in (ORDAZ and SINGH 1992; GARCIA *et al.* 2004); AI07: acceleration spectrum left cutoff data according to (AGUIRRE and IRIKURA 2007, Table 1; left bound of flat acceleration spectral range  $\times 0.7$ ); partly same events as OS92; AI07trend: linear trend for the same data; Ga04 : Mexico intermediate depth/inslab data after (GARCIA *et al.* 2004) **d** Japan and other: KT82: Japan after (KOYAMA *et al.* 1982); Ko94 : 1963 Kurile and 1965 Aleutian great earthquakes,  $f_b \approx 0.16$  Hz after (KOYAMA 1994); CB07: individual great earthquakes based on (CHOY and BOATWRIGHT 2004, 2007); KM90: Japan after (KAMIYAMA and MATSUKAWA 1990); PG99 Kamchatka after (PETUKHIN *et al.* 1999). On each plot, two grey lines are repeated that give the reference trends of the kinds  $f_b \propto M_0^{-1/3}$  (the steeper one, the case of similarity) and  $f_b \propto M_0^{-1/6}$

At magnitudes four and below, simple single-corner spectra are common (see e.g. PRIETO, 2004). This tendency is not obligatory, however, and there exists a certain fraction of small to moderate earthquakes with well separated  $f_a$  and  $f_b$  spectral corners, (see e.g. (RAUTIAN and KHALTURIN, 1978; KINOSHITA and OIKE, 2002).

The first impression from the data shown in Fig. 5 is that  $f_b(M_w)$  trend is not very stable, with varying slope depending on the region and data set. This can be related both to the above-listed problems of  $f_b$  determination, and to the real variability of  $f_b(M_w)$  relationships for different events and regions. Still, one can conclude that the average  $f_b$  versus  $M_0$  trend, when established, is typically slower than  $f_b \propto M_0^{-1/3}$ ; the  $f_b \propto M_0^{-1/6}$  relationship may serve as a plausible first approximation.

Some of the modern engineering-oriented studies assume however similarity of source spectra, i.e.  $f_b$  proportional to  $f_a$ . Still, when the organization of data analysis permits  $f_b$  to vary independently of  $f_a$ , slower  $f_b$  trend is found systematically (see e.g. GARCIA *et al.*, 2004; AGUIRRE and IRIKURA, 2007). One should note that HALLDORSSON and PAPAGEORGIOU (2005), in a thorough study applied to three large data sets came to the conclusion that the barrier interval  $2\rho$ , a critical fault parameter that is inherent in their model, follows the similarity assumption. As  $2\rho$  is directly related to the inverse of  $f_b$ , this conclusion clearly supports the  $f_b \propto f_a$  behavior. Still, one can note that this study is engineering-oriented and no direct spectral fitting was performed in it. Also in a parallel study, BERESNEV and ATKINSON (2002) found  $2\rho \propto M_0^{0.27}$ , slower than  $2\rho \propto M_0^{1/3}$  accepted by

HALLDORSSON and PAPAGEORGIOU (2005). Generally, despite certain supportive evidence, the assumption of similarity in spectral scaling (that requires  $f_b \propto M_0^{-1/3}$ ) is far from being well-established. Numerically, for shallow interplate events,  $f_b$  is around 1.5–2 Hz for  $M_w = 5$  and around 0.25–0.35 Hz at  $M_w = 8$ . Combining these values with usual estimates for  $M_w$  versus fault duration relationship, one can obtain a crude estimate  $f_b/f_a = 2.5$ –12 for the magnitude range 5–8.

In the last two sections, two characteristic spectral features, both located at frequencies  $(3$ – $20) \times$  (common corner frequency), are discussed: the second corner frequency  $f_b$ , and the transitional frequency  $f_{\text{ucoh}}$  that separates the LF spectral range showing clear directivity and HF spectral range with weak directivity (note that for those researchers who do not discriminate between  $f_a$  and  $f_b$ , the second corner is  $f_{\text{max}}$ ). One more characteristic frequency may be associated with local slip duration, or rupture rise time  $T_{\text{rise}}$ ; denote it  $f_{\text{rise}}$ . Following HEATON (1990), one can assume the ratio  $T_c/T_{\text{rise}} = 1/C_H \approx 10$ , where  $C_H \approx 0.1$  is the important dimensionless constant, therefore  $f_{\text{rise}} \approx 10f_c$ . One more possibly relevant parameter is the characteristic duration of the “forward-directivity pulse”  $T_{\text{dir}}$  and related frequency  $f_{\text{dir}} = 1/T_{\text{dir}}$ , approximately,  $T_{\text{dir}} = (0.20$ – $0.25) T_c$  and thus  $f_{\text{dir}} = (4$ – $5) f_c$ . As this pulse represents a coherent signal feature, one can believe that  $f_{\text{ucoh}}$  and  $f_{\text{dir}}$  are close to one another. It is tempting to hypothesize that all these four spectral/temporal features are inherently connected. This has some reason, but no certain conclusion can be presently stated. The  $T_{\text{rise}}$  parameter is difficult to determine without very near-fault observations of fault dislocation, thus no evident association is seen between  $T_{\text{dir}}$  and  $T_{\text{rise}}$  or between  $f_{\text{rise}}$  and  $f_b$ . Still, to associate  $f_b$  with  $f_{\text{rise}}$  seems to be a reasonable idea. It was mentioned by STEIN and WYSESSION (2003), (Sect. 4.6.2) but they do not provide clear arguments to substantiate this guess.

Another relation that looks plausible is one between  $f_b$  and  $f_{\text{ucoh}}$ . It is equivalent to an assumption that it is around  $f_b$  that the radiation style is changing from incoherent one at higher frequencies, to coherent one at lower frequencies. That is, the running strip as a moving HF source displays no intrinsic

directivity; only its LF component, combined with systematic motion along a fault surface, creates LF directivity.

Possible appearance of rupture front that agrees with this idea is discussed later. The assumption that  $f_b$  represents the upper bound of incoherent behavior is physically reasonable because it is equivalent to an assumption that entire acceleration spectrum plateau is homogeneously formed by incoherent radiation.

### 5. Fault-Controlled $f_{\text{max}}$

As mentioned above, acceleration source spectra of moderate to large earthquakes usually show a plateau. This “ $\omega^{-2}$ -style” behavior arises both in cases with  $f_a \approx f_b$ , and when  $f_b$  and  $f_a$  differ significantly so that an intermediate spectral range, roughly of the  $\omega^{-(0.7-1.5)}$  kind, arises between them. The absolute level  $A$  of this plateau plays a crucial role in the determination of strong-motion accelerations, and thus has attracted wide attention. As was found in HANKS and MCGUIRE (1981); BOORE (1983, 1986); BOATWRIGHT (1992); DAN *et al.* (2001) and more, the dependence  $A(M_0)$  mostly follows the  $M_0^{1/3}$  law, just as expected for the constant stress-drop model of BRUNE (1970). It should be noted however that the  $\omega^{-2}$  spectrum behavior of the BRUNE (1970) model follows from a single singularity in the deterministic signal shape that this model generates; whereas the observed random HF signal looks qualitatively differently: as random/stochastic; see GUSEV (2011) for further discussion. No consistent explanation of the stochastic  $\omega^{-2}$  feature has been proposed up to date.

A significant question is whether the source acceleration spectral plateau has any HF cutoff (“source- or fault-controlled  $f_{\text{max}}$ ”), and if yes, where this cutoff is located. This question created a lot of controversy. In the 1980s, PAPAGEORGIOU and AKI (1983) and GUSEV (1983) proposed that empirically well-established  $f_{\text{max}}$  feature (HANKS 1982) is of fault origin. Soon ANDERSON and HOUGH (1984) have convincingly shown however that the conspicuous  $f_{\text{max}}$  feature is commonly caused by near-site constant- $Q$  attenuation in a layer of limited thickness; they used the symbol  $\kappa$  for the corresponding  $t^*$  value. (If  $f_{\text{max}}$  is defined as 50% point of amplitude transfer

function, like common  $f_c$ , then  $\kappa = \log_e 2/\pi f_{\max}$ ). To minimize confusion, two new separate denotations will be further used for the parameters of site-controlled and fault-controlled  $f_{\max}$ ; namely  $f_{us}$ , meaning “upper acceleration spectrum cutoff, site geology-controlled”; and similarly  $f_{uf}$  for the hypothetical fault-controlled cutoff.

The existence of  $f_{us}$  creates a filter for source-generated signal (see Fig. 4) that makes the detection and (if found) estimation of  $f_{uf}$  a complicated problem. Some of the first attempts to estimate  $f_{uf}$  (see e.g. AKI 1988) did not discriminate sufficiently strictly between effects of  $f_{us}$  and  $f_{uf}$ . Other studies (e.g. FACCIOLI 1986) produced quite reasonable starting approximations. To resolve the question and obtain decisive results, two ways were employed for special cases. First, one can use very deep borehole instruments to get rid of  $f_{us}$ -filter effects. KINOSHITA (1992) used data recorded in 2.3 and 3.5 km wells. After path attenuation correction, for two out of five data groups from various sub-volumes he found clear manifestations of  $f_{uf}$  in the range 10–20 Hz; whereas no  $f_{uf}$  was observable for three other groups that showed approximately flat path-corrected acceleration spectra. With the same approach, tens of moderate earthquakes have been analyzed by SATOH (2002) who used 910 m-deep well data. His range for  $f_{uf}$  estimates is mostly 8–20 Hz. Both studies revealed no correlation of  $f_{uf}$  with magnitude; however, SATOH (2002) noticed a clear decrease of observed  $f_{\max}$  with increased stress parameter for a considerable subset of his data. He considers this unexpected tendency as a clear indication that the observed  $f_{\max}$  was of the fault-controlled kind. ATKINSON and BOORE (1995) note that no  $f_{\max}$  phenomenon ( $f_{us}$  or  $f_{uf}$ ) is observed at all for east Canada and Ontario stations up to 20 Hz; this may mean that for this region,  $f_{uf}$  values are typically above 20 Hz. For small earthquakes recorded at the 2.5 km borehole, ABERCROMBIE (1995) also did not notice any indication of  $f_{\max}$  (i.e. of  $f_{uf}$ ) up to 100 Hz for the magnitude range 1–5.

Another possibility to establish reliably the fault origin of  $f_{\max}$  is to find pairs of records of the same station with comparable hypocentral distances, magnitudes and strong motion amplitudes but with markedly unequal  $f_{uf}$ . In such a case, the difference in spectral shapes may be clearly visible, see example in

(GUSEV *et al.* 1997). More systematic approach is to use spectral ratios. For a pair of records of a station, both having flat  $\omega^{-2}$ -type acceleration source spectra, the spectral ratio (path attenuation excluded) must be constant, as the site-controlled factors must cancel. (A station with hard rock ground is preferable for such a study, to minimize possible differences in non-linear attenuation). Therefore, the presence of non-identical  $f_{uf}$  manifests itself as non-constant, ideally, ramp-like, spectral ratio. Such a case was revealed by SASATANI (1997) who found, simultaneously for three digital stations, similar non-flat spectral ratios between two large earthquakes. TSURUGI *et al.* (2008) analyzed spectra of three mainshocks and many aftershocks recorded by KIK-net stations (in boreholes; mostly with depth of about 100 m). Their approach is based, in essence, on spectral ratios, but it is more complicated. They assume true spectra to have, ideally, a preset analytic shape and averaged observed spectra over stations to increase stability. For larger events, they also averaged results for many smaller shocks. Although TSURUGI *et al.* (2008) avoid stating definitely the origin (site vs. fault) of their obtained  $f_{\max}$  estimates, their results suggest to represent  $f_{uf}$ ; this viewpoint is supported by certain magnitude dependence of their  $f_{\max}$  over the magnitude range 3.5–6.5.

The decay of acceleration spectra at HF, parameterized by  $\kappa$ , was studied by PURVANCE and ANDERSON (2003) for a large data set of Mexico accelerograms, with the  $M$  range 3.5–8. Empirical  $\kappa$  estimates were processed by least squares to split them into separate contributions from source ( $\kappa_{\text{event}}$ ) and site ( $\kappa_{\text{site}}$ ). High statistical significance of source contribution was accurately proven. Also, nodal plane solution effect on  $\kappa_{\text{event}}$  was revealed, additionally confirming the reality of source contribution to  $\kappa$ . Significant increase of  $\kappa_{\text{event}}$  with magnitude was found for two of the three frequency bands used for the estimation of  $\kappa$ , however this observation was not considered as an effect of magnitude dependence of the HF upper frequency cutoff of acceleration spectrum. Two other explanations of the mentioned observation are discussed instead: through the effect of magnitude dependence of  $f_b$  of small earthquakes, or through the insufficiently excluded similar dependence of  $f_c = f_a$ . Unfortunately, to make the least squares procedure possible, it was necessary to

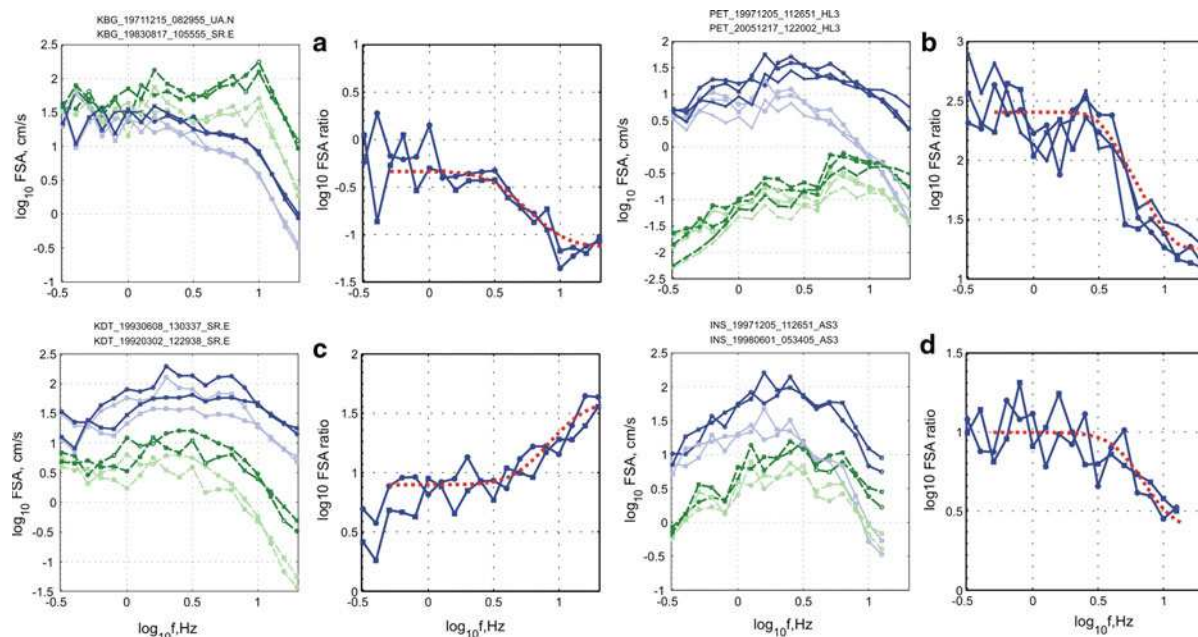


Figure 6

Acceleration spectra and their ratios for accelerograms of Kamchatka earthquakes (see Table 1 for details). Four blocks of graph boxes are shown, each block has Fourier spectra on the *left* and their ratio at the *right*. Spectra are smoothed by 0.1 decade window. Numerator spectra (N): solid grey is original and solid black is path-attenuation corrected (In the color version read “light color” and “dense color” instead of “grey” and “black”). Denominator spectra (D): similar, *dashed lines*. Spectral ratio: solid; its smooth ramp-like approximation—*dotted line*. Component denotation: EW-circle, NZ-square, Z (when shown) -cross. **a** N: 1971.12.15,  $M_w = 7.7$ , D: 1983.08.17,  $M_w = 7.1$ ; station KBG. **b** N: 1997.12.05,  $M_w = 7.9$ , D: 2005.12.17,  $M_w = 4.8$ , station PET. **c** N: 1993.06.08,  $M_w = 7.5$ , D: 1992.03.02,  $M_w = 6.9$ , station KDT. **d** N: 1997.12.05,  $M_w = 7.9$ , D: 1998.06.01,  $M_w = 6.5$ , station PET. Note that in (b) and (d), *left* corners of the ramp function are close to one another (about 3.5–4 Hz), as expected for the case when the numerator event is the same, with certain  $f_{uf}$ . Note also that in cases (a) and (c), the higher  $f_{uf}$  is associated with the event with larger absolute amplitudes, making the explanation through non-linear effects improbable

set the average (over events)  $\kappa_{event}$  contribution equal to zero; thus, it is difficult to judge with certainty about the magnitude of event contribution to total  $\kappa$ . Still, to obtain an order-of-magnitude estimate, one can use the value of LS variance reduction related to the  $\kappa_{event}$  factor, equal to  $(0.0071 \text{ s})^2$ ; this can be translated to the tentative characteristic  $f_{uf}$  value of about 30 Hz.

More results of the spectral ratio approach to  $f_{max}$  analysis applied to a few Kamchatka accelerograms are given here. Examples can be seen on Fig. 6, where one can notice characteristic ramp-like shape of spectral ratios that permits to estimate roughly the value of  $f_{uf}$  for one or, sometimes, for both analyzed earthquakes. In Table 1, estimates of  $f_{uf}$  obtained in this manner are summarized.

Although the spectral ratio technique, especially applied to hard rock data, often efficiently suppresses the biasing effects of  $f_{us}$  and also of site resonances, it

is far from being universal. Even when ramp-like behavior is prominent in the spectral ratio, the higher of the two corners often cannot be established confidently either because of an insufficient work frequency band or because of poorly known path attenuation parameters used for propagation correction, or because of noise contamination of the spectral slope of the weaker event. No reliable information about  $f_{uf}$  can be drawn from frequently seen nearly flat spectral ratio curve, that may indicate either the coincidence of  $f_{uf}$  values of the two events, or the fact that both their  $f_{uf}$  values, even if exist, are above the observable frequency range. Also, there are cases when the ratio of smoothed spectral shapes shows substantial randomly-looking deviations from a flat shape. These can probably be ascribed to peculiarities of individual source spectra that are not covered by simple models of  $f_a-f_b-f_{uf}$  kind; multiple  $f_b$  and/or  $f_{uf}$  models may be necessary.

A significant feature of fault-controlled  $f_{\max}$  operator  $H_{uf}(f)$  is its HF spectral slope. The exponent  $\gamma$  of the law

$$H_{uf}(f) = \frac{1}{[1 + (f/f_{uf})^{2\gamma}]^{0.5}} \quad (12)$$

was found to be about 2.0 by KINOSHITA (1992), SATOH (2002) and about 1.0 by TSURUGI et al. (2008) study. The value  $\gamma = 1.5$  seems to be a good starting approximation for Kamchatka data.

The numerical estimates regarding  $f_{uf}$ - $M$  relationship obtained by the cited authors and also from Table 1 are depicted in Fig. 7. No upper bound is seen for  $f_{uf}$ ; still, data hint to a weak magnitude dependence of  $f_{uf}$ . The apparent slope of the log  $f_{uf}$  versus  $\log M_0$  trend is of the order of 0.1 in accordance with FACCIOLI'S (1986) estimate of 0.12.

The revealed properties of fault-controlled  $f_{\max}$  or  $f_{uf}$  may be summarized in the following way: (1)  $f_{uf}$  feature with  $f_{uf} \leq 25$ -30 Hz is characteristic for a considerable fraction of earthquake faults; (2) for the cases when such  $f_{uf}$  is not observed, the question remains open whether  $f_{uf}$  is non-existent or merely non-observable by modern instrumentation; (3) there is a slight tendency of  $f_{uf}$  to decrease slowly with increasing  $M_0$ .

As for the probable cause of the  $f_{uf}$  phenomenon, one can believe, following PAPAGEORGIOU and AKI (1983), FUJIWARA and IRIKURA (1991) that it is related

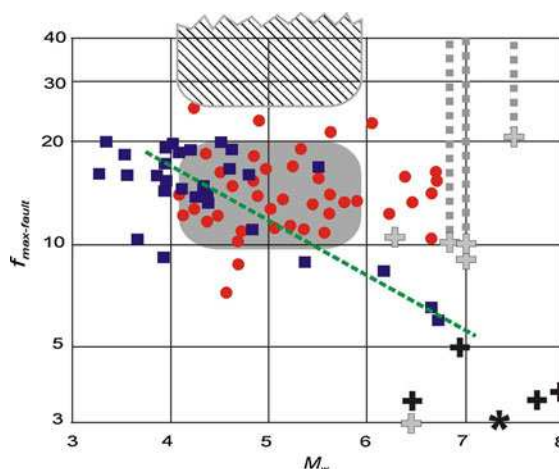


Figure 7

Estimates of  $f_{uf}$  plotted versus  $M_w$  of earthquake. Slant dashed line (green in color) marks the trend after FACCIOLI (1986) for Mediterranean data; it is supported by south Osaka data as cited by YOKOI and IRIKURA (1991). Grey and hatched zones indicate approximately the positions of the results of KINOSHITA (1992) for two groups of seismically active volumes, those with observable  $f_{uf}$  (grey) or with no noticeable  $f_{uf}$  below 30 Hz (hatched). Squares and dots represent, respectively, the results of Sato (2002) and TSURUGI et al. (2008). Star is the estimate derived from the plot of SASATANI (1997). Crosses show Kamchatka data as given in Table 1, better quality in black and lower quality in grey. A cross with tail shows the case when only the lower bound of  $f_{uf}$  can be determined

to the existence of upper wavenumber limit of rupture front propagation details defined, e.g., by crack cohesion length. Alternatively, GUSEV (1990) associated  $f_{uf}$  with the upper wavenumber limit (and  $1/f_{uf}$

Table 1

Approximate estimates of fault-controlled  $f_{\max}$ , or  $f_{uf}$ , for larger Kamchatka earthquakes, as obtained with the spectral ratio technique

Date (year/mo/day)	Lat. °N	Long. °E	Depth, km	Mw	Station	Soil	$r_{\text{hypo}}$	Instrument	$f_{uf}$ , Hz*
1971/12/15	55.85	163.35	25	7.7	KBG	Stiff	80**	UAR	3.5 A
1983/08/17	55.64	161.53	98	7.1	KBG	Stiff	120	SSRZ	>10 L
1984/12/28	56.18	163.45	25	6.9	KBG	Stiff	50	SSRZ	>10 L
2001/08/02	56.20	164.05	25	6.3	KBG	Stiff	87	ASZ	11 L
1992/03/02	52.76	160.22	35	6.9	KDT	Stiff	167	SSRZ	5 A
1993/06/08	51.20	157.83	40	7.5	KDT	Stiff	80	SSRZ	>20 L
1996/01/01	53.88	159.44	15	6.4	SPN	Rock	81	SSRZ	3.5 A
1993/11/13	51.79	158.83	40	7.1	PET	Rock	143	FBA	9 L
1996/01/01	53.88	159.44	15	6.4	PET	Rock	110	FBA	3.0 L
1997/12/05	54.64	162.55	35	7.9	PET, INS	Rock, Stiff	240**	FBA, SSRZ	3.5 A, 4 A

\* A denotes acceptable and L denotes lower quality estimate

\*\* Approximate distance to the source centroid

with lower fractal limit) of random, assumedly fractal, composite topography of fault interface. Following GUSEV (1989), this topography is believed to be related to formation of multiple random contact patches—small asperities—where the fault strength is concentrated. These patches occupy only a limited fraction, 2–10%, of the nominal contact area; the remaining part of the fault has negligible strength. For the case of fractal topography, most contact patches must be small, with characteristic size defined by the mentioned fractal limit. No deep physical meaning is ascribed to this characteristic size; its formation is associated with the abrasion and wear of fault walls. Abrasion selectively suppresses smaller asperities by grinding off smaller hills of the composite topography faster than larger ones (GUSEV, 1990; MATSUURA, 1992; SAGY *et al.*, 2007); wear creates a gouge layer that is capable to “plaster off” smaller asperities. Therefore, typically, the younger is the active fault wall interface, the smaller is the minimum wavelength of the composite profile, and the higher is  $f_{uf}$ . Therefore, at a first glance, one can expect close correlation between the cumulative offset of a geological fault and  $f_{uf}$ . This main tendency may be significantly counterbalanced, however, by the fact that for an active geological fault, consequent ruptures often propagate intermittently along sub-parallel branches that can be reactivated or formed anew. Therefore, even in a mature fault zone, a significant part of the active interface area of a particular earthquake may be sufficiently young. Still, certain limited correlation between  $f_{uf}$  and cumulative offset can be expected. A further line of reasoning is as follows. The cumulative fault offset is positively correlated with fault length (e.g. RANALLI 1980), fault length with rupture length, and the latter with magnitude. The last steps of reasoning introduce additional uncertainty because there are cases of multiple-segment ruptures formed by joining separate geological faults, as well as ruptures spanning only a limited section of a single geological fault. Still, certain limited degree of positive correlation between  $f_{uf}$  and magnitude can be expected. The two listed explanations for  $f_{uf}$  (through characteristic cohesion length and through lower limit for contact patch size) need not be considered as mutually exclusive; actually, they may well be complementary.

Recently, the effect of abrasion and wear of fault wall composite topography with cumulative fault offset, and therefore with magnitude was assumed to be a cause of relative decrease of levels of HF radiation from three  $M \approx 7.5$  earthquakes as compared to smaller-magnitude earthquakes (ANDERSON 2002). This viewpoint is strongly supported by clear average trends of “local stress drop” parameter that slowly decreases with magnitude, as found by HALLDORSSON and PAPAGEORGIOU (2005) for two out of three large sets of accelerograms analyzed. Reasoning in a similar way, PURVANCE and ANDERSON (2003) tentatively propose the observed difference in their  $\kappa_{event}$  estimates between thrust (mostly interslab) and normal (mostly intraslab) events to be connected to relatively smaller cumulative offset for the latter group. Indeed, abrasion of fault walls may produce both effects on parallel: reduce the amplitudes of composite topography and thus average amplitudes of HF radiation; and at the same time decrease the upper wavenumber cutoff of this topography, and  $f_{uf}$  with it.

## 6. Heavy-Tailed Statistics of HF Amplitudes

HANKS and MCGUIRE (1981) proposed “regular” Gaussian statistics for near-fault accelerogram amplitudes and, in essence, for source-radiated HF signal. Oppositely, GUSEV (1989) noticed that conspicuous spikes are often present in near-fault acceleration traces and on this basis proposed very heavy tailed statistics for HF signal. Observations show a large variability in the degree of spiky behavior of accelerograms, from moderate (see Fig. 1) to prominent, as exemplified by Fig. 8.

In terms of power-law approximation for complementary cumulative distribution function (CCDF) of acceleration peaks  $A_p$ , GUSEV (1989) proposed that the tail of CCDF is of the kind

$$P(A'_p > A_p) \sim A_p^{-\alpha} \quad (13)$$

with  $\alpha$  around two. The hypothesis of very heavy-tailed HF amplitudes is supported by LAVALLEE and ARCHULETA (2003), LAVALLEE *et al.* (2006) who believe that  $\alpha$  is close to one. However, such low values for  $\alpha$  as 1–2 seemingly predict too heavy tails

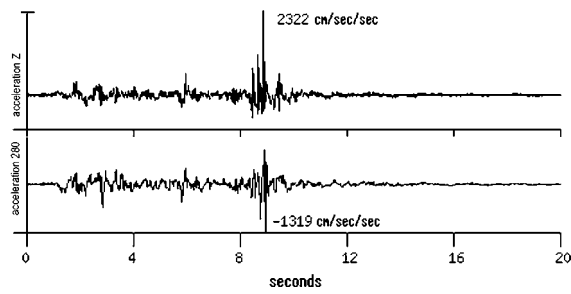


Figure 8

Acceleration traces (horizontal 280° and Z) of very near-fault record of 1986.12.23,  $M_w = 6.7$ , Nahanni, Canada, earthquake illustrate prominently non-Gaussian amplitude statistics. Station “Site1”, hypocentral distance about 10 km

for CCDF of acceleration amplitudes, requiring acceleration signals to be excessively spiky.

Indeed, although GUSEV (1996) established rather reliably that accelerations peaks observed on near-fault accelerograms of large-magnitude Mexican earthquakes do have non-Gaussian heavy-tailed statistics, he obtained relatively moderate upper estimate of  $\alpha = 4-5$ . GUSEV (1996) also have shown that the data cited by HANKS and MCGUIRE (1981) in support of their Gaussian-behavior hypothesis actually show deviations from the Gaussian law, and point again to a similar heavier-tailed law. For teleseismic HF amplitudes, GUSEV (1992) derived  $\alpha \approx 2.3-2.7$  from the  $m_b$  versus  $M_w$  relationship, but his argumentation was rather indirect. Using a direct approach, less prominent estimates  $\alpha = 3-4.5$  were found for tails of CCDF of amplitudes of teleseismic HF  $P$ -wave trains of large earthquakes (Gusev, manuscript in preparation). The range of  $\alpha = (2.5-4)$  seems to represent a reasonable preliminary estimate for near-fault conditions. At a distance, somewhat larger values of  $\alpha$  can be expected because along-path scattering must systematically modify the distribution of the signal, suppressing the tails and making it closer to the Gaussian one; this “normalization” tendency can be directly seen in local data (GUSEV 1996).

A particular prominent acceleration or velocity spike can be also considered individually/deterministically, not as a statistical outburst. Two approaches were proposed to explain their formation. The first approach is to depart from intrinsic fault structure. HANKS and JOHNSON (1976) have associated prominent acceleration peaks with the failure of high-stress-drop

spots on the fault surface. One can believe, therefore, that local peaks in time functions must be related to local stress drop statistics in space. High-strength asperity model of DAS and KOSTROV (1983) provided a solid theoretical basis to this idea. From this model, one can expect a failing asperity to produce a characteristic one-sided velocity pulse and the presence of such a pulse in real data might be considered as a confirmation of this concept, see GUSEV (1989) for discussion and examples. More examples of a similar kind are given on Fig. 9. Another explanation for formation of a prominent observed acceleration spike (rather complementary than alternative) is through constructive interference of amplitudes formed by a deterministic arcuate converging rupture front (OGLESBY and ARCHULETA 1997).

### 7. Fractal HF Envelopes

Recently, stochastic structure of envelopes of source-generated HF radiation has been systematically analyzed (GUSEV 2010). The subject of analysis was squared band-filtered time histories of HF teleseismic  $P$ -waves of large,  $M_w = 7.6-9.2$ , earthquakes. In other words, instant power signal was analyzed and estimated separately for a few HF spectral bands. Such signals look highly intermittent, with bursts and fadings; they evidently deviate from a primitive signal model of stationary constant-variance random noise modulated by a smooth envelope function. One may try to describe quantitatively this burst behavior in terms of random fractals. This approach was found to be valid: fractal or self-similar behavior was successfully revealed. This result was obtained both for recorded signals (at a station) and, with less abundant data, for reconstructed radiated signals (at a source).

Two methods were employed that are standard in establishing fractal features of time functions: analysis of variograms and of power spectra (see Fig. 10 for example). The standard variogram technique was slightly modified, so as to produce constant-level modified variograms for the reference case of non-fractal, white noise signal. Similarly, flat power spectra are expected in this case. Almost all observed modified variograms show clear positive slope in the

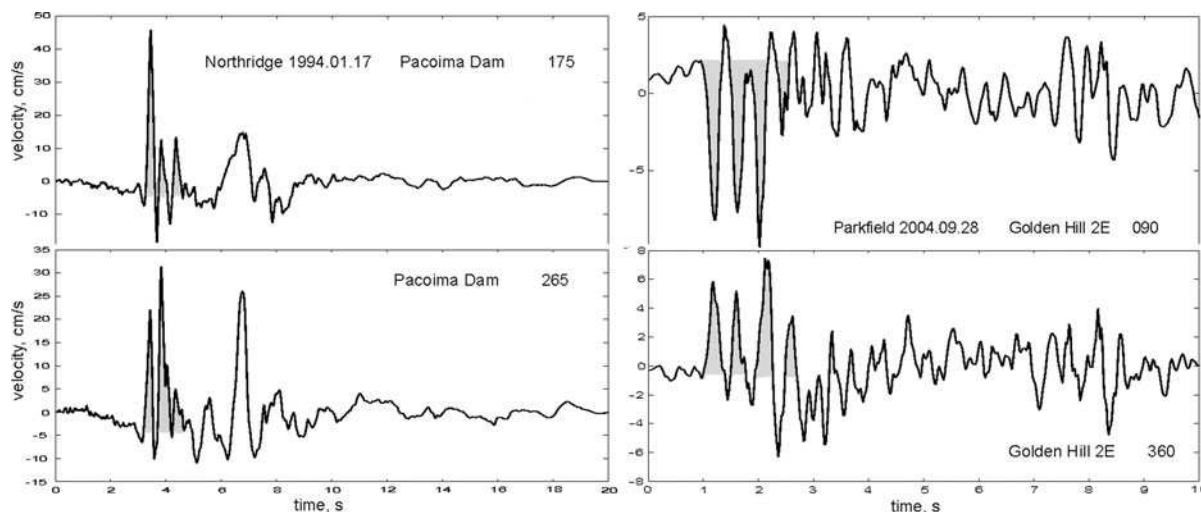


Figure 9

Examples of clear one-sided velocity spikes probably related to the failure of individual small asperities. For event, station and component see lettering on the plot

log–log scale, indicating self-similar correlation structure of the signal. Also, power spectra of the instant power signal show (negative) linear slope in log–log scale ( $1/f^\alpha$  behavior), again indicating self-similarity. Still, slight systematic deviations from a simple fractal behavior were found and also minor discrepancies between the results of two methods; therefore, the result of the described study was formulated as the “approximately fractal behavior”. The standard parameter to specify a fractal behavior is the Hurst exponent  $H$ ; its value can be directly calculated from the log–log slope of variogram or spectrum. The related single-trace estimates of the Hurst exponent  $H$  are mostly in the range 0.6–0.9.

In the analysis of fractal properties of seismological data, there is an important complication related to low accuracy of estimates. Unfortunately, with the actual balance of frequency content and duration of earthquake signals, estimates of  $H$  based on a single trace inevitably show large scatter, and occasional expressed deviations occur. This problem is akin to the “small sample” difficulty in common statistics. For this reason, to prove convincingly the fractal behavior, and to obtain stable estimates of  $H$ , results for many individual records and frequency bands were averaged, see Fig. 11 for example. Stable  $H$  estimates were obtained for nine earthquakes using data of 10–57 stations. The preferred average value of

$H$  equals 0.83, based on power spectra. Inter-event standard deviation of estimates of  $H$  is about 0.05, probably reflecting slight individual variation of  $H$  among earthquakes.

Employing teleseismic  $P$ -wave data, fractal behavior of envelopes could be established only for HF signals within a limited frequency range of 1–6 Hz. To broaden this range, one can analyze  $S$ -wave trains represented by near-fault accelerograms. Also, near-fault data are free from propagation-related (multipathing and scattering) distortion inherent in teleseismic signals. In Figs. 12, 13, preliminary results of such a study are illustrated. The frequency band of signals that show the features of fractal behavior was expanded up to 20–25 Hz. All the features revealed for teleseismic  $P$ -wave data manifest themselves also with accelerogram data.

The analysis of fractal structure of accelerograms also creates a sound basis for adequate simulation of the temporal structure of HF strong motion. There is a well-known representation of an accelerogram as a segment of stationary noise with a smooth envelope function. This model may serve as an initial approximation, but it is clearly oversimplified. This is evident if one compares bursty envelopes of real signals (Figs. 12b, 13) with similar envelopes for artificial white noise (Fig. 12a). This qualitative judgment is well supported numerically by the values

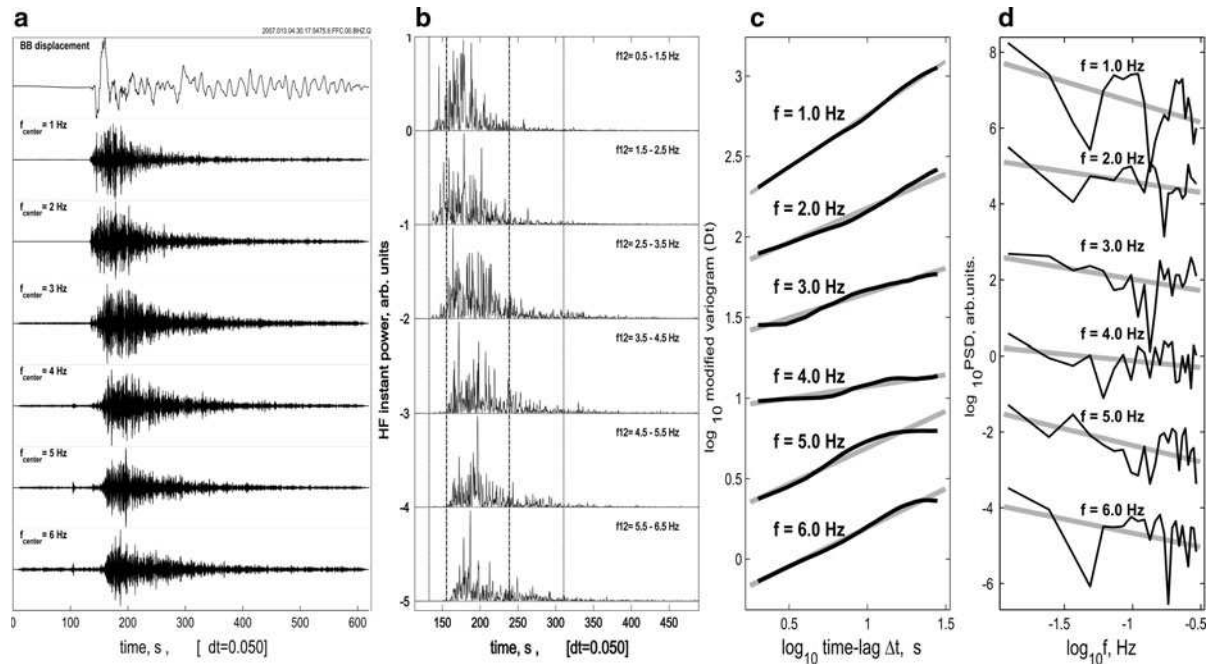


Figure 10

Examples of variograms and power spectra of envelopes of band-filtered HF teleseismic  $P$ -waves. Plots are given for the 2007.01.13,  $M = 8.2$ , Kurile Isles, event as recorded by station FFC (BHZ). **a** BB displacement (the uppermost trace) and six filtered traces of  $P$ -waves with frequency bands  $1 \pm 0.5$ ;  $2 \pm 0.5$ ; ... ;  $6 \pm 0.5$  Hz. **b** Instant power of the filtered traces of **a**. **c** Modified variograms and **d** power spectra of the central segment of data shown in **c**, with linear fit shown in grey; their slopes can be converted to estimates of the Hurst exponent  $H$

of the Hurst exponent: around 0.5 for the white noise, as compared to 0.65–0.9 for real data.

### 8. Models of Generation of HF Radiation

It seems relevant here to give a very short review of conceptual models that have been proposed to explain the properties of HF radiation see GUSEV (2011) for a larger review with an accent on engineering application). Housner (1955) realized the noise-like and broadband character of accelerograms and explained it quite sensibly as produced by a multitude of randomly fired dislocations-components of the main earthquake source. These sub-dislocations were assumed to have broad, power-law-shaped distribution of sizes, with sub-dislocation number proportional to (dislocation area)<sup>-1</sup>. This view was further developed by Blandford (1975) and Hanks (1979). It is not a simple task to distribute sub-dislocations or subsources over the fault area. Boatwright (1982) proposed to cover the main-

shock source area by crack-like subsources arranged in one layer abutting one another, with subsource perimeters partly broken and partly unbreakable. A similar arrangement with cracks of identical sizes with an unbreakable perimeter was proposed by Aki (1977) and successfully tested against large-earthquake data by Papageorgiou and Aki (1983, 1985); for a close concept see also Beresnev and Atkinson (1999). Zeng *et al.* (1994) cover fault surface by several layers of populations of circular cracks with hierarchy of sizes; such a construct is less attractive geomechanically but more versatile. Koyama (1985, 1994) proposed a single-layer model of non-overlapping fault patches with a special size distribution that was proposed to explain complicated, “humpy” spectral shapes of Koyama *et al.* (1982), Gusev (1983) or Izutani (1984). An advanced and geomechanically more admissible model of this kind is one after Irikura and Kamae (1994) who proposed a hierarchy of abutting cracks surrounded by barriers that first stand for awhile and then break.

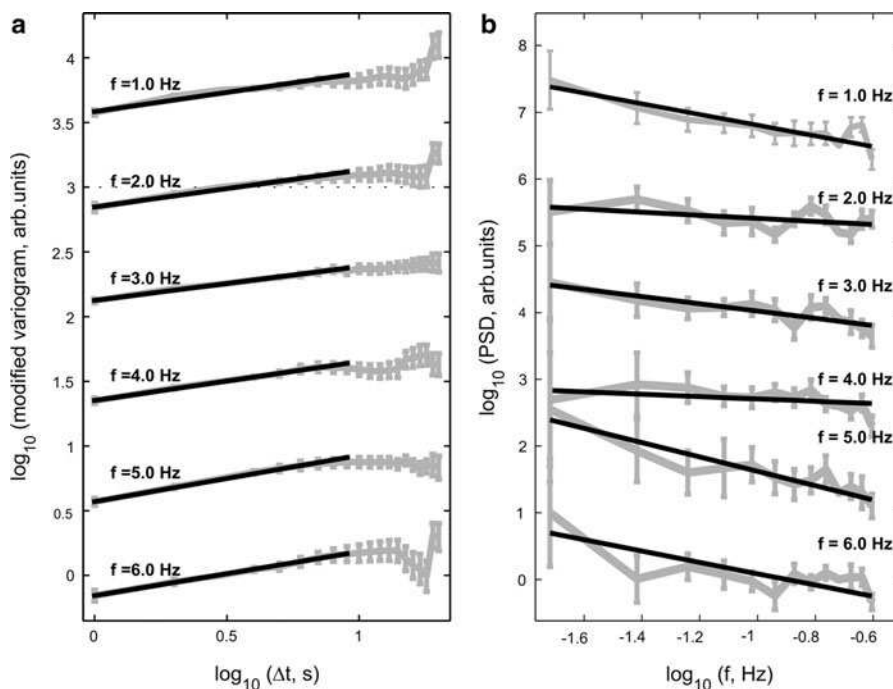


Figure 11

Average modified variograms and power spectra of envelopes of band-filtered HF teleseismic  $P$ -waves of the 2007.01.13,  $M = 8.2$ , Kurile Isles, event; obtained by stacking 17 single-station estimates like Fig. 10 cd. **a** grey: variograms; black: linear fit, its slope provides  $H$  estimate; **b** similar plot for power spectra

In difference with all these models, GUSEV (1989) associated HF seismic signals not to subcracks but to small asperities (“strength asperities”, strong patches over the fault surface) of the kind proposed by DAS and KOSTROV (1983, 1988). These asperities were thought to occupy only a small part (2–10%) of the nominal surface of the fault interface; they are dispersed over a weak background that covers most of the surface. To form a jumping, multiply-connected rupture propagation mode, strength contrast of fault spots must be considerable, and must show itself as heavy-tailed statistics of strength of fault patches (asperity and non-asperity patches merged together). This tendency must and does show itself as similar statistics of HF signal amplitudes as discussed above. The concept of composite-asperity fault was also put forward by BOATWRIGHT (1988) but in difference with (GUSEV 1989) his asperities are tightly packed; they tile the fault area and are neither separated by low-strength background nor have a heavy-tailed distribution of strength. Small strong asperities are

tectonophysically highly plausible because the contact of rough fault walls can be expected to create just this kind of strength distribution. Dynamics of multiple-asperity fault was simulated in the instructive model of DAS and KOSTROV (1988). Only recently have the asperities of this kind been revealed in fault inversion (DREGER *et al.* 2007) though the general understanding of this phenomenon was already achieved by HANKS and JOHNSON (1976). An important attractive feature of the multi-asperity fault is that it is geomechanically transparent and does not need to assume unbreakable barriers or repeated, multiple failure of points of a fault. There is a difference between the multi-asperity fault concept and the asperity concept of LAY and KANAMORI (1981): although the governing mechanics is essentially the same, the organization of the rupture is qualitatively different: many randomly fired small patches in the multi-asperity model as compared to small number of relatively large areas whose failure is a deterministic process creating no incoherence. The difference may

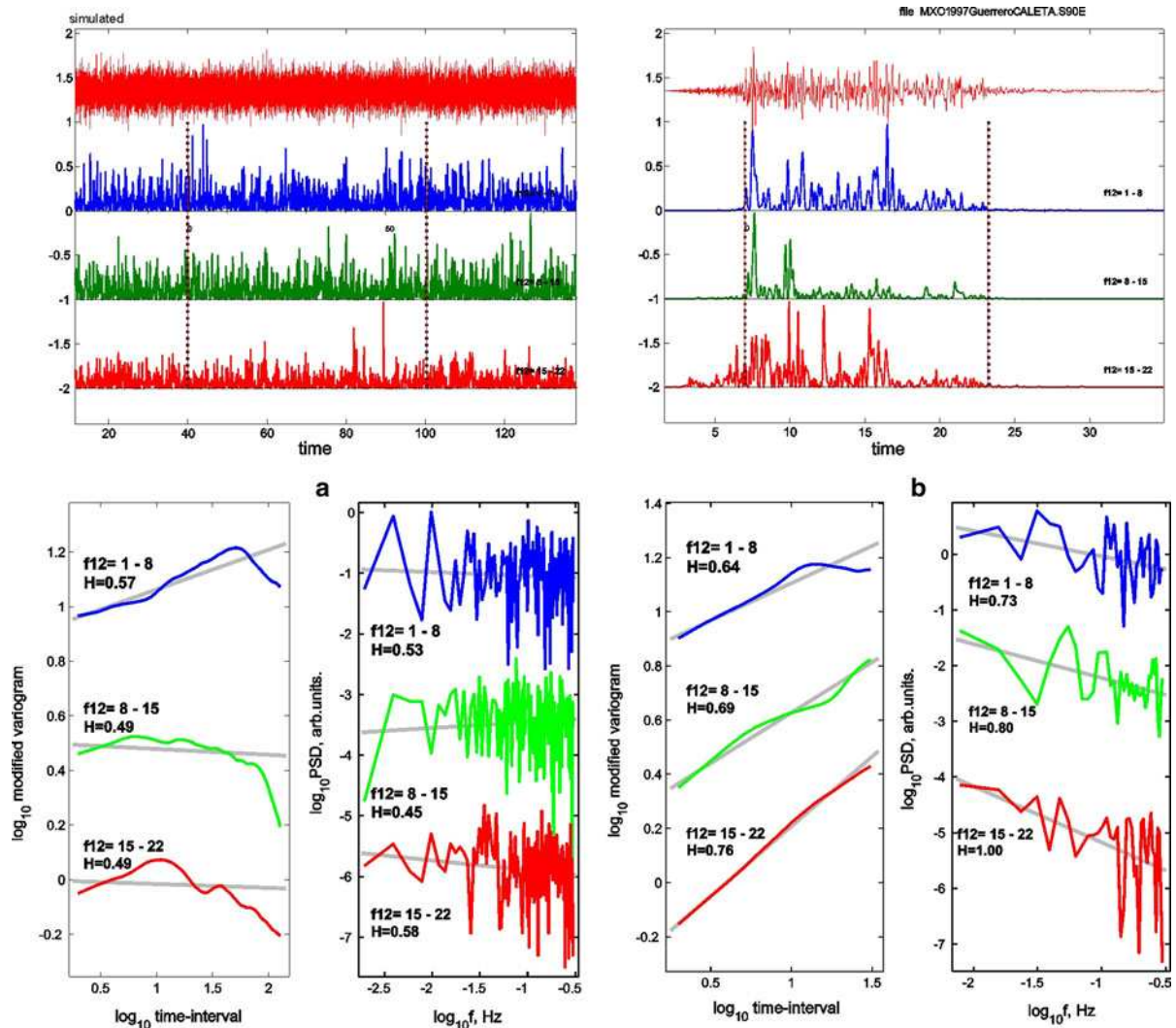


Figure 12

Examples of modified variograms and power spectra of envelopes of band-filtered accelerograms. Two blocks (a) and (b), each of three *graph boxes*, show results: **a** for a white noise test signal, **b** for *E* component of the digital record of the 11 January 1997,  $M = 7.0$ , Guerrero, Mexico earthquake by the station CALE, the hypocentral distance is about 50 km. In each block, the *top box* shows the input trace and instant power traces for the frequency bands, and *vertical lines* indicate the segment processed; the *left bottom box* shows modified variograms and the *right bottom box* shows power spectrum density (PSD). *Grey lines* are linear approximations. Bands and estimates of  $H$  are indicated by lettering. With stationary white noise input signal (*case a*) both modified variogram and PSD plots are nearly horizontal, with no significant dependence correspondingly, on time lag or on frequency. Oppositely, well-expressed slopes are seen in modified variograms and PSD for each band of real data, reflecting the fractal structure of envelope time functions

be not fundamental however because “large deterministic” asperities of LAY and KANAMORI (1981) may represent aggregates or clusters of “small stochastic” asperities of GUSEV (1989).

To elucidate the properties of an assumed multi-asperity fault and to explain the related broad-band spectral structure, GUSEV (1989) introduced two scales—“macro”-scale and “micro”-scale. He proposed

to consider an earthquake source, situated on a fault with multiple small asperities, as a “macroscopic” shear crack. (The mechanism of asperity formation was discussed above in relation to fault-controlled  $f_{\max}$ ). During rupture formation, its front propagates “macroscopically smoothly”. “Microscopically”, however, the propagating rupture is a wave or signal that turns on, with random additional delays, breaking

of small asperities. In other words, when examined at low resolution, a fragmented rupture front is indistinguishable from an ideal brittle crack tip with a single well-defined singularity: both look similarly if only long wavelengths are analyzed. Whereas at high resolution, the revealed pictures are qualitatively completely different. One can believe that a fragmented rupture front is a characteristic feature of a real earthquake process on small space–time scales. An important feature of this concept is very natural formation of incoherence of HF radiation. This concept will be further discussed and illustrated below.

From the viewpoint of HF or broadband earthquake signal generation, an adequate rupture model may represent a random fractal. As for spatial structure, an important composite fractal fault model was proposed by FRANKEL (1991); a similar model was proposed by AKI and IRIKURA (1991) as referenced in YOKOI and IRIKURA (1991). IRIKURA and KAMAE (1994) propose certain spatio-temporal organization; they assume crack-like subsources to form a hierarchical or fractal structure in space, with smaller-scale objects that are organized in clusters (not homogeneously). Each crack-cluster, when viewed at a reduced resolution, represents a unit subsource at the next structure level. Alternatively, fractal fault structure can be composed of multiple-scaled, hierarchically clustered strong asperities on a weak background, as discussed above, c.f. GUSEV (1992). This paper includes also a fault model composed of chains of small strong asperities; this concept originates in a hierarchical fractal barrier grid model of FUKAO and FURUMOTO (1985). The scale dependence of asperity strength, in a fractally clustered multiple-asperity fault model was examined by SAMMIS *et al.* (1999); they underline that the smallest asperities must be very strong (in the kilobar range). All fractally structured fault models are basically of exploratory value; still, they try to grasp correlated fractal space–time structure that may eventually provide an efficient description of fault structure and rupture evolution.

Although the stochastic models of incoherent HF radiator consisting of multiple individual subsources may look reasonable, in essence they are rather speculative. Particularly, they lose reliability if

applied in the vicinity of a fault. Indeed, at fault distances smaller than subsource size, a subsource must be treated in non-random fashion, and a conceptual incompatibility arises. Models that describe fault evolution through random functions of space–time (HASKELL 1966; ANDREWS 1981) raise more hope in this respect. Along this line, GUSEV and PAVLOV (2009); [see also GUSEV (2011)] developed a model of an incoherently radiating fault represented as a grid of nodes with no physical meaning, that produce HF signals with no directivity and controllable correlation. To fix the spectral properties and amplitudes for the nodes, they calibrate the energy spectrum of such a source using assumedly known broad-band far-field spectrum. To meet requirements of a particular application, the cell size of the grid of nodes can be adjusted, so as to account for the minimum site-to-fault-plane distance needed. This approach permits, in principle, to simulate ground motion at distances as close as 1–2 km from fault interface.

#### 9. Joint Analysis of the Listed Properties of HF Radiation: the Hypothesis of Fractal Structure of a Rupture Front

In the previous section it is hypothesized that the running strip where the slippage is localized generates incoherent HF radiation with no intrinsic directivity, whereas as a whole it moves as an organized entity and, in particular, is capable to generate the LF feature of the “forward directivity pulse”. A systematic illustration of this concept would demand simulation of a complete space–time rupture history that follows the described concept. In the following, a more limited aim is pursued—to simulate example geometry of a rupture front.

To provide incoherence and no HF directivity, the rupture front at small characteristic distances or at high wavenumbers  $k$ , ( $k = |k| = (k_x^2 + k_y^2)^{0.5}$ ) must represent a line (typically, a multiply connected line or “polyline”) with randomly directed normal. The smoothed version of the same front (its low- $k$  version) must however be single-connected and follow the common organized, locally unilateral mode of propagation. One simple possibility to provide such properties is to assume that there is a lot of

elementary sources or subevents, such that any particular individual subevent either has no preferred local rupture-propagation direction (random symmetry), or represent a deterministically symmetric rupture. These subevents are ignited by a “switch-on” signal that propagates with certain velocity and commands a subevent to nucleate. Often nucleation happens not immediately but with some random delay, added to the signal-arrival time in order not to create fully deterministic LF directivity. This is how the PAPAGEORGIOU and AKI (1983) model is organized, where subevents are symmetrically propagating circular cracks. Oppositely KOYAMA (1985) assumed that each his patch has a certain definite direction of local rupture propagation (and therefore directivity) but these directions are randomized for a population of patches, and the symmetry is maintained on the average. The multiple-subevent models have already been criticized above. In the following paragraph, a more systematic approach is developed with respect to front geometry. The generation procedure will be fully kinematic, with no dynamics included. Still, even such a model seems useful because the incoherent fault behavior is rather difficult to visualize.

To simulate realistically-looking rupture front, one has to combine discontinuous propagation mode at high wavenumbers (that results in random directivity) with organized, systematic propagation (and expressed directivity) at low wavenumbers. The proposed simple model assumes that the rupture onset time  $t_{\text{on}}(x, y)$  at a point  $(x, y)$  of a rectangular  $L \times W$  fault is

$$t_{\text{on}}(x, y) = R(x, y) + S(x, y) \quad (13)$$

with two terms. The first term  $R(x, y)$  is random; it supplies all discontinuous, tortuous high- $k$  structure of the front.  $R(x, y)$  is assumed to be self-similar or fractal, with zero mean. The second term is non-random and provides systematic behavior at low  $k$ . Assume mean rupture to propagate from a hypocenter, e.g. at a constant velocity along radius  $r$  at velocity  $v_{\text{rup}}$ , then  $S(x, y) = r/v_{\text{rup}}$ . The approach expressed by (13) has much common with that proposed by HISADA (2000); the critical and significant difference is that in Hisada’s concept, the rupture front evolves monotonously and no random backward motion of the (local) front is assumed, only its acceleration and deceleration. In the present

Figure 13

More examples of modified variograms and power spectra of envelopes of band-filtered accelrograms. Four *blocks of graph boxes* are shown, each block is organized as in Fig. 12b. They show results: **a, b** for  $E$  and  $N$  components of the analog record of intermediate-depth 24 November 1971,  $M = 7.6$ , Kamchatka, earthquake, by station PET, hypocentral distance about 120 km; **c, d**—for  $E$  and  $N$  components of the record of 26 September 2003,  $M = 8.2$ , Hokkaido earthquake by digital borehole instrument OSMH02 of KIKnet, hypocentral distance about 100 km. See Fig. 12 for explanation

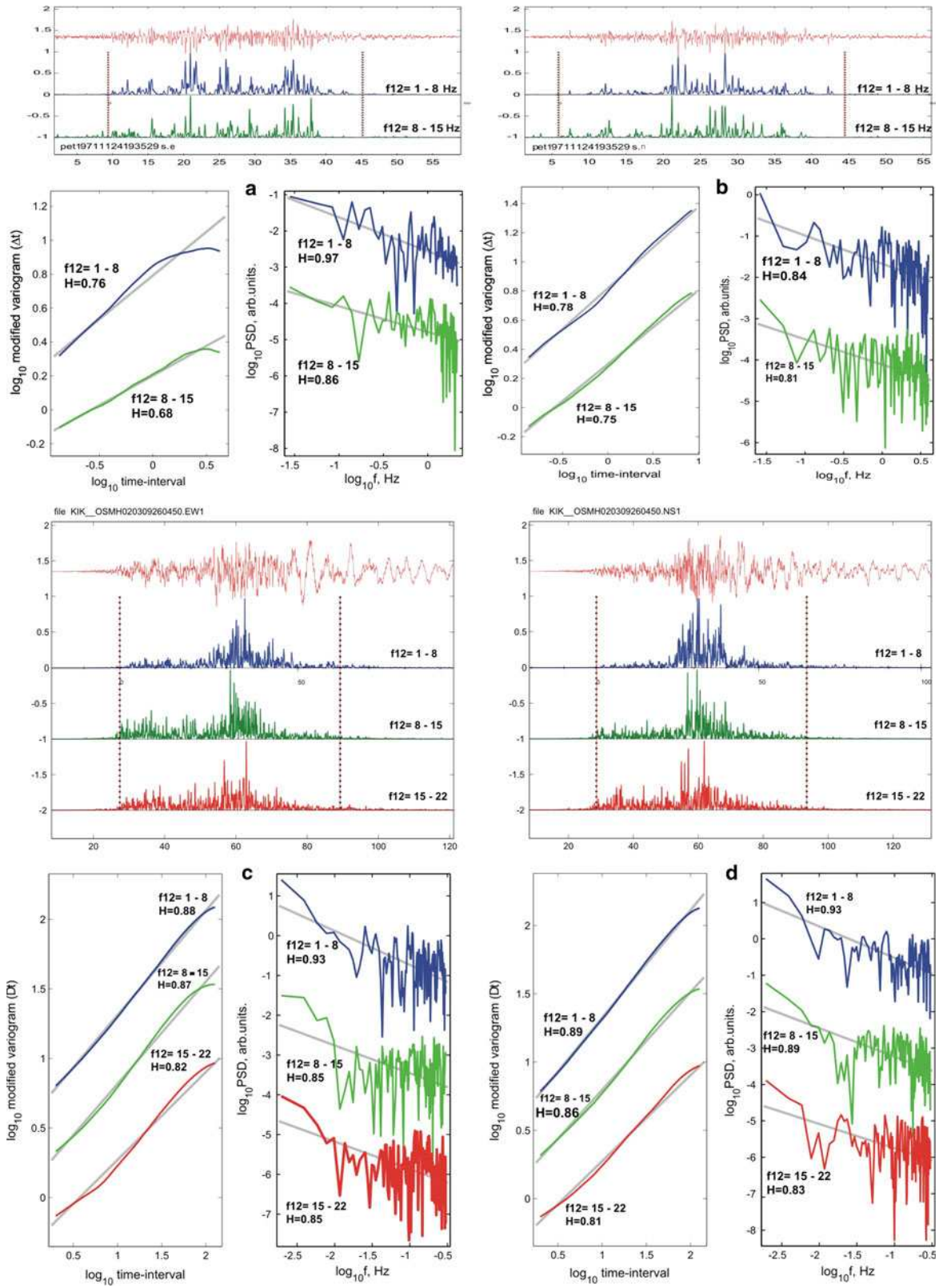
approach, randomly omnidirectional local front propagation is considered crucial because only in this way the HF directivity can be effectively suppressed.

The locally random front normal (local propagation direction) is generated automatically. By selection of appropriate parameters for  $R(x, y)$  one can simulate a front geometry that is discontinuous and multiple-connected, with controllable degree of expression of these properties. Particularly, a lot of localized “lakes” and “islands” can be generated. These can be called in military terms as “jumping-off grounds” ahead of the mean front line, and as “residual resistance centers” in the rear.

Figure 14 is a graphical illustration generated to illustrate these ideas. The map on the left shows the full range of wavenumbers; still certain high- $k$  limit ( $k_{\text{max}}$ , set about half of the Nyquist  $k$ ) is set to make the smallest details discernible. The inverse of this limit,  $k_{\text{max}}^{-1}$ , can be considered from different viewpoints as: lower fractal limit, coherence length, or minimum asperity size. The map on the right shows only the lowermost wavenumbers. It shows smooth curved fronts that bear no interesting randomness. Under these maps, time-distance plots are shown. On the left plot, a non-monotonous manner of propagation is well seen, with the range of random fluctuations of the front arrival time of the order of 10% of the complete propagation time, as intended for the case of  $C_H = 0.1$ .

A very short historical reference must be made. The seemingly earliest example of high-stress fault patch that nucleates before the arrival of rupture front to it, giving a basic structure for fragmented, multiply-connected rupture, is seen on Fig. 13 of DAY (1982). Also, models with fractal geometry of rupture front has been proposed, e.g. a percolation-cluster kinematic rupture after LOMNITZ-ADLER and LUND (1992);

HF Earthquake Radiation: Review and Fractal Rupture Front



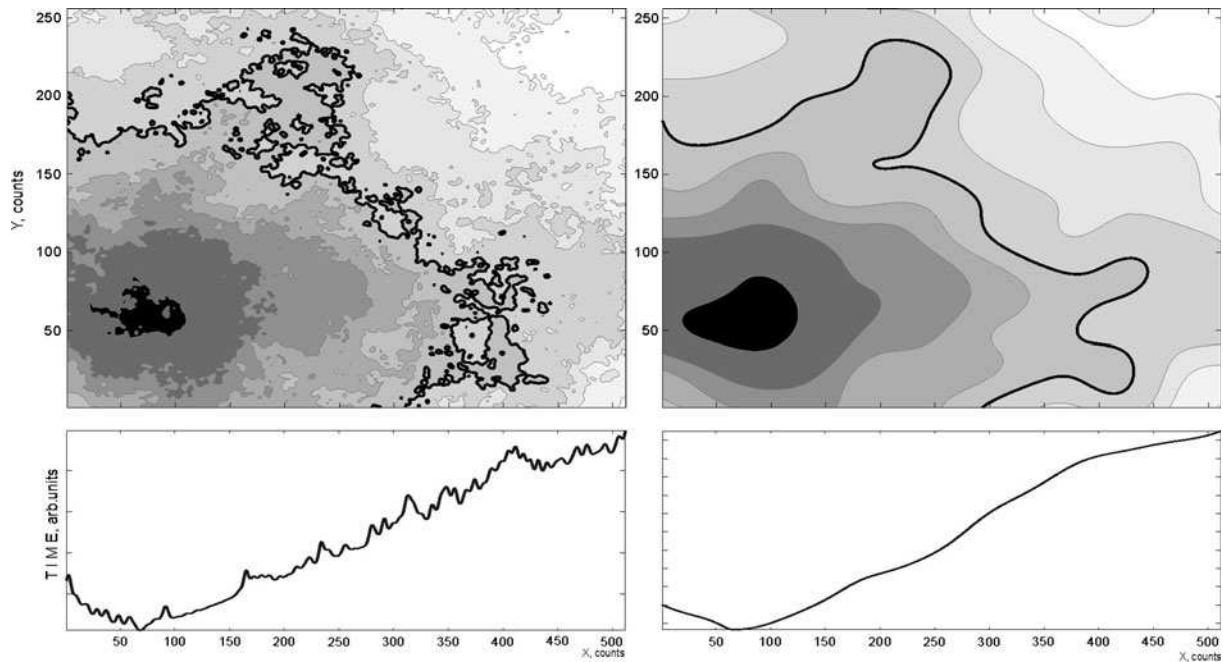


Figure 14

Fault maps depicting hypothetical rupture evolution represented as a sequence of fractal isolines that show instant positions of the rupture front (*top left*). *Black* spot encircles the hypocenter; shades of *grey* represent time (the lighter, the later). The *black line*, tortuous and multiply connected, depicts a particular example instant position of the hypothetical rupture front; its timing is arbitrary and was selected to provide graphical clarity. At the *top right*, the smoothed variant of the same map is shown. Under the maps, corresponding plots for the arrival time of the rupture front are plotted for the line  $y = 60$ . Note non-monotonous dependence of onset time versus distance for the unsmoothed map; it is this non-monotonous behavior that generates random phases of contributions of fault spots at a receiver, creating incoherence

but in this case, no “jumping-off grounds” are permitted, whereas “residual resistance centers” or local unbroken barriers are generated in excessive abundance. Another, more realistic looking, is the random rupture front generated by quasistatic simulation of a fracture in damaged material after SILBERSCHMIDT (2000). In this case, the width of a “thick” random rupture front grows with its travel distance. Thus, there is no need in this model to artificially introduce the rise time-rupture length correlation. SILBERSCHMIDT (2000), however, does not consider the problem of incoherence.

### 10. Conclusions

(A) Observed HF radiation from earthquake faults has important specific features, namely

1. Recorded HF time histories have a random appearance which suggests that ruptures

behave non-deterministically at small space-time scales. HF signals have non-Gaussian probability density, with (moderately) heavy distribution tails, manifested as occasional prominent acceleration spikes. These spikes probably reflect non-Gaussian, heavy-tailed statistics of local stress drops over a fault surface.

2. The propagation-related directivity of HF energy radiation is deteriorated or absent as compared to that of LF energy; this fact indicates incoherent behavior of HF radiator. Such behavior suggests irregular/fragmented/multiply-connected geometry of rupture front at high wavenumbers.
3. The general shape of source spectrum includes three characteristic frequencies: traditional corner  $f_c \equiv f_a$ , the second corner  $f_b$  and the upper corner “fault-controlled  $f_{max}$ ” or  $f_{uf}$ . Acceleration spectrum is flat between  $f_b$  and  $f_{uf}$  forming the well-known  $\omega^{-2}$  spectral

behavior. Between  $f_a$  and  $f_b$ , the spectral trend is, very roughly,  $\omega^{-1}$ . The common “single-corner” assumption ( $f_a = f_b$ ) is actually valid only in a fraction of cases; for larger-magnitude events it often represents an oversimplification. The tradition to determine “stress parameter” from the intersection of extrapolated branches:  $\propto \omega^0$  at  $f < f_a$  and  $\propto \omega^{-2}$  at  $f > f_b$  may be tolerable in engineering applications as a compact empirical representation of average spectral properties, but this “stress parameter” has no immediate physical meaning by itself. Outside engineering applications, the tendency to determine in this manner the single  $f_c$  value may be misleading, producing incorrect geophysical estimates both for stress drop and for fault size. Any systematic study of spectral shape must assume the presence of two corners ( $f_a$  and  $f_b$ ), in accordance with the original BRUNE (1970) assumption regarding spectral shapes; these parameters typically differ for moderate-to-large magnitude earthquakes.

4. The observed data on the  $f_b$  ( $M_0$ ) relationship show certain trend, with variations from region to region and from the average-stress-drop to the high-stress-drop earthquake subpopulations. If this trend is approximated as  $f_b \propto M_0^\gamma$  one might use  $\gamma = 1/6$  as an initial approximation for its exponent, in significant difference with  $\gamma = 1/3$  predicted by the spectral similarity hypothesis.
5. The upper cutoff of source acceleration spectrum, “fault-controlled  $f_{max}$ ”, or  $f_{uf}$ , is very rarely observable directly because of the masking effect of the site-controlled upper spectral cutoff,  $f_{us}$ . However, the presence of  $f_{uf}$ , often in the range 3–25 Hz, can be revealed in a significant fraction of analyzed cases when special means of registration or processing are employed. In particular, spectral ratios permit to suppress effects both of site-controlled  $f_{max}$  and site resonances, and turned to be an efficient (though not universal) tool for extraction information regarding  $f_{uf}$ . Still, the general amount of

accumulated  $f_{uf}$  observations is scarce. In a significant fraction of cases, there are substantial deviations of real source acceleration spectra from the ideal scheme of relatively broad “ $\omega^{-2}$ ” plateau bounded by two corners  $f_b$  and  $f_{uf}$ . Data on  $f_{uf}$  tentatively suggest its slow decrease with magnitude; this trend is seen on the background of large scatter and is not quite certain.

6. Random-looking time histories of HF (1–20 Hz) radiation generated by propagating earthquake ruptures consistently show self-similar correlation structure of instant power. This fractal behavior has been revealed both for teleseismic  $P$  wave and near-fault  $S$ -wave records. One can imply that earthquake rupture process that generates such signals is multiple-scaled itself, with fractal features; it cannot be reduced to smooth brittle crack propagation with 2–3 well-separated characteristic scales. The  $f_b$ – $f_{uf}$  spectral plateau can be associated with the spectral range of incoherent radiation and of (band-limited) fractal behavior. Therefore,  $f_{uf}$  may provide estimates of the upper fractal limit of the above-mentioned rupture front geometry.
- (B) Considered in their entirety, the described features permit to state the following hypothesis. The instant position of a propagating rupture front may be idealized as a random “line” or polyline, tortuous and, generally, multiply connected, with randomly directed normal. This “line”, or polyline, represents a random fractal. This line is “thick”, i.e. it occupies a finite strip whose width is of the order  $l = T_{rise} v_{rup}$ . At wavelengths smaller than  $l$ , i.e. at high frequencies, this fragmented polyline structure, with multiple “islands” and “lakes”, serves as an incoherent radiator and thus efficiently suppresses propagation-related directivity of radiation. At wavelengths longer than  $l$ , i.e. at low frequencies and low spatial resolution, the polyline of the rupture front looks as a traditional linear object with well defined velocity and, locally, definite propagation direction.

## Acknowledgments

The following open Internet sources of data and graphics are gratefully acknowledged: IRIS DMC [<http://www.iris.edu/data/>]; KiK-net data center [<http://www.kik.bosai.go.jp/kik/quake/>] and COSMOS data center [<http://db.cosmos-eq.org/scripts/search.plx>]. The paper is based on the invited talk at the 7th ACES Workshop at Otaru, Japan, 2010; author is very grateful to its organizers for their kind invitation. Comments of an anonymous reviewer helped to improve the manuscript.

## REFERENCES

- ABERCROMBIE, R. E. (1995). *Earthquake source scaling relationships from 1 to 5 M L using seismograms recorded at 2.5 km depth*, J. Geophys. Res. 100, 24015–24036.
- ABRAHAMSON, N. A. (2000). “Effects of rupture directivity on probabilistic seismic hazard analysis.” Sixth International Conference on Seismic Zonation, Earthquake Engineering Research Inst., Oakland, California.
- AGUIRRE, J., and IRIKURA, K. (2007). *Source characterization of Mexican subduction earthquakes from acceleration source spectra for the prediction of strong ground motions*, Bull Seismol Soc Am, 97, 1960–1969. doi:10.1785/0120050156.
- AKI, K. (1972). *Scaling law of earthquake source-time function*, Geophys. J. Roy. Astron. Soc. 31, 3–25.
- AKI, K. (1967). *Scaling law of seismic spectrum*, J Geophys Res, 72, 1217–1231.
- AKI, K., (1988) Physical theory of earthquakes, in Seismic Hazard in Mediterranean Region, ed. J. BONONIN, M. CARA, M. CISTERNAS, R. FANTECHI, Kluwer Academic Publ., 3–34.
- AKI, K. and K. IRIKURA (1991). Characterization and mapping of earthquake shaking for seismic zonation. In: Proceedings of the Fourth International Conference on Seismic Zonation, Vol. I, pp. 61–110.
- AKI, K., et al. (1977). *Quantitative prediction of strong motion for a potential earthquake fault*. Ann. Geofis. 30, 81–91.
- ANDERSON, J. G., HOUGH, S. E. (1984). *A model for the shape of the Fourier amplitude spectrum of acceleration at high frequencies*, Bull Seismol Soc Am, 74, 1969–1993.
- ANDERSON, J. G., J. N. BRUNE, S. G. WESNOSKY (2002). Physical phenomena controlling high-frequency seismic wave generation in earthquakes, in Proc. of the 7th U.S. National Conf. on Earthquake Engineering, Boston.
- ANDREWS, D. J. (1981). *A stochastic fault model, 2: time-dependent case*, J Geophys Res, 86, 10831–10834.
- ATKINSON, G. (1993). *Source spectra for earthquakes in eastern North America*, Bull. Seism. Soc. Am. 83, 1778–1798.
- ATKINSON G. and BOORE D.M. (1995) Ground-Motion Relations for Eastern North America by Gail M. Atkinson and David M. Boore Bulletin of the Seismological Society of America, vol. 85, No. 1, pp 17–30, February 1995.
- ATKINSON G. and BOORE D.M. (1998) New Ground-Motion Relations for Eastern North America by Gail M. Atkinson and David M. Boore Bulletin of the Seismological Society of America, vol. 85, No. 1, pp 17–30, February 1995.
- ATKINSON, G., and W. SILVA (2000). *Stochastic modeling of California ground motions*, Bull. Seism. Soc. Am. 90, 255–274.
- ATKINSON, G., and W. SILVA (1997). *Empirical source spectra for California earthquakes*, Bull. Seism. Soc. Am. 87, 97–113.
- BAKUN W. H., R. M. STEWART and C. G. BUFE (1978) *Directivity in the high-frequency radiation of small earthquakes*. Bull Seismol Soc Am. 68, 1253–1263.
- BEN-MENACHEM A. (1961) *Radiation of seismic surface-waves from finite moving sources*; Bull. seism. Soc. Am v. 51; no. 3; p 401–435.
- BEN-MENACHEM, A. (1962), *Radiation of Seismic Body Waves from a Finite Moving Source in the Earth*, J. Geophys. Res., 67(1), 345–350, doi:10.1029/JZ067i001p00345.
- BERESNEV, I. A. and ATKINSON, G. M. (1999), *Generic finite-fault model for ground-motion prediction in Eastern North America*, Bull Seismol Soc Am, 89, 608–625.
- BERESNEV, I., and G. ATKINSON (2002). *Source parameters of earthquakes in eastern and western North America based on finite-fault modeling*, Bull. Seism. Soc. Am. 92, 695–710.
- BLANDFORD, R. R. (1975), *A source theory for complex earthquakes*, Bull Seismol Soc Am, 65, 1385–1405.
- BOATWRIGHT, J. (1982). *A dynamic model for far-field accelerations*, Bull. Seism. Soc. Am. 72, 1049–1068.
- BOATWRIGHT J (1988); *The Seismic Radiation From Composite Models Of Faulting*, Bull Seism Soc Am, 78, 489–508.
- BOATWRIGHT J. (2007) *The Persistence of Directivity in Small Earthquakes*, Bull Seismol Soc Am, 97, 1850–1861.
- BOATWRIGHT, J. and H. QUIN (1986). The seismic radiation from a 3-D dynamic of a complex rupture process, in *Earthquake Source Mechanics, Geophysical Monograph 37, Maurice Ewing Series*, vol. 6, S. DAS, J. BOATWRIGHT, and C. H. SCHOLZ, Editors, American Geophysical Union, Washington, D.C., 97–109.
- BOATWRIGHT, J., and G. L. CHOY (1989). *Acceleration spectra for subduction zone earthquakes*, J. Geophys. Res. 94, 15,541–15,553.
- BOATWRIGHT, J., and G. L. CHOY (1992). *Acceleration source spectra anticipated for large earthquakes in northeastern North America*, Bull. Seism. Soc. Am. 82, 660–682.
- BOORE, D. M. and W. B. JOYNER (1978). *The influence of rupture incoherence on seismic directivity*, Bull. Seism. Soc. Am. 68, 283–300.
- BOORE, D. M. (1986). *Short-period P- and S-wave radiation from large earthquakes: implications for spectral scaling relations*, Bull. Seism. Soc. Am. 76, 43–64.
- BOORE, D. M. (1983), *Stochastic simulation of high-frequency ground motions based on seismological models of radiated spectra*, Bull Seism Soc Am, 73, 1865–1894.
- BOORE, D. (2003). *Prediction of ground motion using the stochastic method*, Pure Appl. Geophys. 160, 635–676.
- BRUNE, J. (1970). *Tectonic stress and the spectra of seismic shear waves from earthquakes*, J. Geophys. Res. 75, 4997–5009.
- CASTRO R R., FRANCESCHINA G, PACOR F, BINDI D and LUZI L (2006) Analysis of the Frequency Dependence of the S-Wave Radiation Pattern from Local Earthquakes in Central Italy. 96, 415–426; doi:10.1785/0120050066.
- CHOY G. L. and J. BOATWRIGHT (2004) *Radiated Energy and the Rupture Process of the Denali Fault Earthquake Sequence of 2002 from Broadband Teleseismic Body Waves* Bull. seism. Soc. Am 94. S269–S277.

- CHOY G. L. and J. BOATWRIGHT (2007) *The Energy Radiated by the 26 December 2004 Sumatra–Andaman Earthquake Estimated from 10-Minute P-Wave Windows* Bull. seism. Soc. Am 97, S18–S24, doi:10.1785/0120050623.
- DAN, K., WATANABE, T., SATO, T., and ISHII, T. (2001), *Short-period source spectra inferred from variable-slip rupture models and modeling of earthquake fault for strong motion prediction*, J Struct Constr Eng AIJ, 545, 51–62.
- DAS, S., and KOSTROV, B. V. (1983), *Breaking of a single asperity: rupture process and seismic radiation*, J Geophys Res, 88, 4277–4288.
- DAS, S., and KOSTROV, B. V. (1988), *An investigation of the complexity of the earthquake source time function using dynamic faulting models*, J Geophys Res, 93(B7), 8035–8050.
- DAY, S. (1982), *Three dimensional simulation of spontaneous rupture: The effect of non-uniform pre-stress*, Bull. Seismol. Soc. Am., 72, 1881–1902.
- DAY, S. M., GONZALEZ, S. H., ANOOSHEHPOOR, R., and BRUNE, J. N. (2008), *Scale-model and numerical simulations of near-fault seismic directivity*, Bull Seismol Soc Am, 98, 1186–1206. doi: 10.1785/0120070190.
- DREGER, D., NADEAU, R. M., and CHUNG, A. (2007), *Repeating earthquake finite source models: strong asperities revealed on the San Andreas Fault*, Geophys Res Lett, 34, L23302. doi: 10.1029/2007GL031353.
- FACCIOLI E. 1986. A study of strong motions from Italy and Yugoslavia in terms of gross source properties, in S. DAS, J. BOATWRIGHT, C. SCHOLZ (Eds.): Earthquake source mechanics, Geophys. Monograph 37, M. Ewing Vol. 6, Am. Geophys. Union, Washington, pp. 297–310.
- FRANKEL A (1991) *High frequency spectral falloff of earthquakes, fractal dimension of complex rupture, b values, ad scaling of strength on faults*. J. Geophys. Res 96, 6291–6302.
- FUJIWARA H and K. IRIKURA (1991) High-frequency seismic wave radiation from antiplane cohesive zone model and fmax as source effect. Bulletin of the Seismological Society of America, Vol. 81, No. 4, pp. 1115–1128.
- FUKAO, Y. and M. FURUMOTO. (1985). *Hierarchy in earthquake size distribution*. Phys. Earth Planet. Interiors 37, 35–148.
- GALLOVIC, F. and J. BURJANEK (2007) *High-frequency directivity in strong ground motion modeling methods*. Ann. Geophysics, 50, 203–211.
- GARCIA, D. S. K. SINGH, M. HERRAIZ, J. F. PACHECO, and M. ORDAZ (2004) *Inslab Earthquakes of Central Mexico: Q, Source Spectra, and Stress Drop*. Bull Seismol Soc Am; 94, No. 3, 789–802.
- GUSEV, A. A. (1983), *Descriptive statistical model of earthquake source radiation and its application to an estimation of short-period strong motion*, Geophys J R Astr Soc, 74, 787–808.
- GUSEV, A. A. (1989), *Multiasperity fault model and the nature of short-period subsources*, Pure Appl Geophys, 130, 635–660.
- GUSEV A.A. (1990) On relations between asperity population and earthquake population on a fault. Extended Abstract. International symposium on earthquake source physics and earthquake precursors. University of Tokyo, Bunkyo-ky, Tokyo. P. 140–142; accessible at <http://www.emsd.ru/~gusev>.
- GUSEV, A. A. (1992) *On relations between asperity population and earthquake population on a fault*. Tectonophysics, 211, 85–98.
- GUSEV, A. A. (1996), *Peak factors of Mexican accelerograms: evidence of non-Gaussian amplitude distribution*, J Geophys Res, 101, 20083–20090.
- GUSEV A. A. (2010) *Approximate Stochastic Self-Similarity of Envelopes of High-Frequency Teleseismic P-Waves from Large Earthquakes*. Pure Appl. Geophys. 167, 1343–1363.
- GUSEV A.A. (2011) *Broadband Kinematic Stochastic Simulation of an Earthquake Source: a Refined Procedure for Application in Seismic Hazard Studies*. Pure Appl. Geophys. doi:10.1007/s00024-010-0156-3.
- GUSEV, A. A., and PAVLOV, V. M. (1991), *Deconvolution of squared velocity waveform as applied to study of non-coherent shortperiod radiator in earthquake source*, Pure Appl Geophys, 136, 235–244.
- GUSEV, A. A. E. I. GORDEEV, E. M. GUSEVA, A. G. PETUKHIN and V. N. CHEBROV (1997) *The First Version of the Amax(MW, R) Relationship for Kamchatka*. Pure appl. geophys. 149, 299–312.
- GUSEV, A. A., and PAVLOV, V. M (2009), *Broadband simulation of earthquake ground motion by a spectrum-matching, multiple-pulse technique*, Earthq Spectra, 25, 257–276.
- GUSEV, A. A., and SHUMILINA L. S. (2000), *Modeling the intensity-magnitude- distance relation based on the concept of an incoherent extended earthquake source*, Vulc Seis, 21, 443–463 (English edition; original in Russian: (1999) 4–5, 29–40).
- GUSEV, A. A., GUSEVA, E. M., and PANZA, G. F. (2006), *Correlation between local slip rate and local high-frequency seismic radiation in an earthquake fault*, Pure Appl Geophys, 163(7), 1305–1325. doi:10.1007/s00024-006-0068-4.
- HALLDORSSON, B., and PAPAGEORGIOU A. S. (2005), *Calibration of the specific barrier model to earthquakes of different tectonic regions*, Bull Seism Soc Am, 95, 1276–1300. doi:10.1785/0120040157.
- HANKS, T. C. (1982)  $f_{\max}$  Bull Seism Soc Am, 72; 1867–1879.
- HANKS, T. C. (1979), *b values and omega-gamma seismic source models: Implication for tectonic stress variations along active crustal fault zones and the estimation of high-frequency strong ground motion*, J Geophys Res, 84, 2235–2242.
- HANKS, T. C. and JOHNSON, D. A. (1976), *Geophysical assessment of peak accelerations*, Bull. Seismol.Soc. Amer. 66, 959–968.
- HANKS, T. C., and MCGUIRE, R. K. (1981), *The character of high frequency strong ground motion*, Bull Seism Soc Am, 71, 2071–2095.
- HASKELL, N. A. (1964). *Total energy and energy spectral density of elastic wave radiation from propagating faults*, Bull Seismol Soc Am, 54, 1811–1841.
- HASKELL, N. A., (1966), *Total energy and energy spectral density of elastic wave radiation from propagating faults. II. A stochastic fault model*. Bull Seism Soc Am, 56, 125–140.
- HEATON, T. H., (1990), *Evidence for and implications of self-healing pulses of slip in earthquake rupture*, Phys Earth Planet Inter, 64, 1–20.
- HERRERO, A., and BERNARD, P. (1994), *A kinematic self-similar rupture process for earthquakes*, Bull Seism Soc Am, 84, 1216–1228.
- HISADA Y (2000) *A theoretical omega-squared model considering the spatial variation in slip and rupture velocity*, Bull Seism Soc Am, 90, 387–400.
- HOUSNER, G. W. (1955), *Properties of strong ground motion earthquakes*, Bull Seismol Soc Am, 45, 197–218.
- IRIKURA, K., KAMAE, K., (1994) Estimation of strong ground motion in broad-frequency band based on a seismic source scaling model and an empirical Green's function technique. Annali Di Geofisica, 37, 6, pp 1721–1743.

- IZUTANI, Y. (1984) *Source parameters relevant to heterogeneity of a fault plane*. J. Phys Earth, 32, 511–529.
- JOHNSON J.M., TANIOKA Y., SATAKE K., RUFF L.J. (1995). Two 1993 Kamchatka earthquakes, 144, 633–647, 0033-4553/95/040633-1551.50 + 0.20/0.
- JOYNER W (1991). *Directivity for non-uniform ruptures*. Bull Seismol Soc Am.; 81: 1391–1395.
- KAMIYAMA M., MATSUKAWA T. (1990) An empirical scaling of strong-motion spectra with application to estimate of source spectra. Struct. Eng/Earthquake Eng, v 7, 331–342.
- KANAMORI, H., and ANDERSON, D. L. (1975), *Theoretical basis of some empirical relations in seismology*, Bull Seism Soc Am, 65, 1073–1095.
- KINOSHITA, S. (1992). *Local characteristics of the  $f_{max}$  of bedrock motion in the Tokyo metropolitan area, Japan*, J. Phys. Earth, 40, 487–515.
- KINOSHITA S. and OIKE M. (2002) *Scaling Relations of Earthquakes That Occurred in the Upper Part of the Philippine Sea Plate beneath the Kanto Region, Japan, Estimated by Means of Borehole Recordings* Bull Seism Soc Am 92, 611–624.
- KOSTROV, B. V. (1974) *Mechanics of the source of a tectonic earthquake*. (Nauka Moscow) (in Russian).
- KOYAMA J., TAKEMURA M. and SUZUKI Z. (1982) A scaling model for quantification of earthquakes in and near Japan Tectonophysics, 84, 3–16.
- KOYAMA, J. (1985). *Earthquake source time-function from coherent and incoherent rupture*, Tectonophysics 118, 227–242.
- KOYAMA J., IZUTANI Y. (1990) *Seismic excitation and directivity of short-period body waves from a stochastic fault model*, Tectonophysics 175, 67–79.
- KOYAMA J. (1994) *General description of the complex faulting process and some empirical relations in seismology*, J.Phys. Earth, 42, pp.103–148.
- LAVALLEE, D., and ARCHULETA, R. (2003). *Stochastic modeling of slip spatial complexities for the 1979 Imperial Valley, California, earthquake*, Geophys Res Lett, 30, 1245. doi:10.1029/2002GL015839.
- LAVALLEE, D., LIU, P. -CH., and ARCHULETA, R. J. (2006) *Stochastic model of heterogeneity in earthquake slip spatial distributions*, Geophys J Int, 165, 622–640. doi:10.1111/j.1365-246X.2006.02943.x.
- LAY, T. and H. KANAMORI (1981). As asperity model of large earthquake sequences, in: *Earthquake Prediction—An International Review, Maurice Ewing Series*, vol. 4, D. SIMPSON and P. G. RICHARDS, Editors, American Geophysical Union, Washington, D.C., 579–592.
- LIU H.L. and HELMBERGER D.V. (1985) *The 23:19 aftershock of the 15 October 1979 Imperial Valley earthquake: More evidence for an asperity* Bull Seism Soc Am. 75, 689–708.
- LOMNITZ-ADLER, J. and F. LUND (1992) *The generation of quasi-dynamical accelerograms from large and complex seismic fractures*. Bull. Seismol. Soc. Am., 82, 61–80.
- MANIC M. (2004) *Scaling laws for Fourier acceleration spectra in former Yugoslavia*. 13th World Conference on Earthquake Engineering Vancouver, B.C., Canada, Paper No. 2682.
- MAVROEIDIS, G. P., and A. S. PAPAGEORGIOU (2003). *A mathematical representation of near-fault ground motions*, Bull. Seismol. Soc. Am. 93, 1099–1131.
- MATSU'URA, M., H. KATAOKA and B. SHIBAZAKI, 1992, *Slip-dependent friction law and nucleation processes in earthquake rupture*, Tectonophysics, 211, 135–148.
- NAKAHARA, H. (2008) *Seismogram envelope inversion for high frequency seismic energy radiation from moderate-to-large earthquakes*, Adv Geophys, 50, 401–426.
- OGLESBY D. D., ARCHULETA R. J. (1997). *A faulting model for the 1992 Petrolia earthquake: Can extreme ground acceleration be a source effect?* J Geophys Res, 102(B6), 11.877–11.897.
- OHNO, S., OHTA, T., IKEURA, T., and TAKEMURA, M. (1993) *Revision of attenuation formula considering the effect of fault size to evaluate strong-motion spectra in near field*, Tectonophysics, 218, 69–81.
- ORDAZ, M., and SINGH, S. K. (1992), *Source spectra and spectral attenuation of seismic waves from Mexican earthquakes, and evidence of amplification in the hill zone of Mexico City*, Bull Seismol Soc Am, 82, 24–43.
- PAPAGEORGIOU A. S. 1988. *Seismological Society of America On two characteristic frequencies of acceleration spectra: patch corner frequency and  $f_{max}$* . Bull Seismol Soc Am; 78; 2; 509–529.
- PAPAGEORGIOU, A. S., and AKI, K. (1983), *A specific barrier model for the quantitative description of inhomogeneous faulting and the prediction of the strong ground motion, I: Description of the model*, Bull Seismol Soc Am, 73, 693–722.
- PAPAGEORGIOU, A. S., and AKI, K. (1985) *Scaling law of far-field spectra based on observed parameters of the specific barrier model*, Pure Appl Geophys, 123, 354–374.
- PETUKHIN, A. G. A. A. GUSEV, E. M. GUSEVA, E. I. GORDEEV and V. N. CHEBROV (1999). *Preliminary Model for Scaling of Fourier Spectra of Strong Ground Motion Recorded on Kamchatka*. Pure appl. geophys. 156 445–468.
- PRIETO, G. A., P. M. SHEARER, F. L. VERNON, D. KILB. (2004), *Earthquake source scaling and self-similarity estimation from stacking P and S spectra*, J. Geophys. Res., 109, B08310, doi: 10.1029/2004JB003084.
- PURVANCE M. D. and J. G. ANDERSON (2003) *A Comprehensive Study of the Observed Spectral Decay in Strong-Motion Accelerations Recorded in Guerrero, Mexico* Bull. Seismol. Soc. Amer, 2003; 93; 2; 600–611; doi:10.1785/0120020065.
- RANALLI G., 1980, *A stochastic model for strike-slip faulting*. Math.Geol.12, 399–412, doi:10.1007/BF01029423.
- RAUTIAN T.G. and V.I. KHALTURIN (1978) *The use of the coda for determination of the earthquake source spectrum*. Bull. Seismol. Soc. Am., 68; 923–948.
- ROGERS A. M. and D. M. PERKINS (1996) *Monte Carlo simulation of peak-acceleration attenuation using a finite-fault uniform-patch model including isochrone and extremal characteristics* v. 86; no. 1A; p. 79–92.
- ROWSHANDEL B. (2006) *Incorporating Source Rupture Characteristics into Ground-Motion Hazard Analysis Models*. Seism. Res. Lett. 77, 708–722.
- ROWSHANDEL, B. (2010). *Directivity correction for the Next Generation Attenuation (NGA) relations*, Earthq. Spectra 26, 525–559.
- SAGY, A., E. E. BRODSKY and G. J. AXEN. (2007). *Evolution of fault-surface roughness with slip*. Geology,; 35, 283–286; doi: 10.1130/G23235A.1.
- SAMMIS C.G., NADEAU R.M., and JOHNSON L.R. (1999). *How strong is an asperity?* J. Geophys. Res. 104 (B5): 10609–10619.
- SASATANI, T., (1997). *Source characteristics of the 1994 Hokkaido Toho-oki earthquake deduced from wide band strong-motion records*. J. Fac. Sci. Hokkaido Univ. Ser. VII (Geophys.) 10, 269–293.

- SATO, T., 2002. *Empirical frequency-dependent radiation pattern of the 1998 Miyagiken-Nanbu earthquake in Japan*, Bull. seism. Soc. Am., 92(3), 1032–1039.
- SEEKINS L. C. and J. BOATWRIGHT (2010) *Rupture Directivity of Moderate Earthquakes in Northern California*. Bull Seismol Soc Am, 100: 1107–1119.
- SHEBALIN N.V. (1974) Sources of strong earthquakes on the territory of USSR. Moscow, Nauka., pp 42–43, [in Russian].
- SILBERSCHMIDT, V. V. (2000) *Dynamics and scaling characteristics of shear crack propagation*, Pure Appl Geophys, 157, 523–538.
- SINGH, S. K., M. ORDAZ, J. G. ANDERSON, M. RODRIGUEZ, R. QUAAS, E. MENA, M. OTTAVIANI, and D. ALMORA (1989). *Analysis of near-source strong-motion recordings along the Mexican subduction zone*. Bull. Seismol. Soc. Amer, Vol. 79, No. 6, pp. 1697–1717.
- SOMERVILLE, P.G., (1998). Development of an improved representation of near fault ground motions. In: Proceedings of the SMIP98 Seminar on Utilization of Strong Ground Motion Data, Oakland, California, pp. 1–20.
- SOMERVILLE, P. G., 2003. *Magnitude scaling of the near fault rupture directivity pulse*, J. Phys. Earth Planet. Interiors 137, 201–212.
- SOMERVILLE, P. G., N. F. SMITH, R.W. GRAVES, and N. A. ABRAHAMSON (1997). *Modification of empirical strong ground motion attenuation relations to include the amplitude and duration effects of rupture directivity*, Seismol. Res. Lett. 68, 199–222.
- SPUDICH, P. and D. OPPENHEIMER (1986). Dense seismograph array observations of earthquake rupture dynamics, in *Earthquake Source Mechanics, Geophysical Monograph 37, Maurice Ewing Series*, vol. 6, S. DAS, J. BOATWRIGHT, and C. H. SCHOLZ, Editors, American Geophysical Union, Washington, D.C., 285–296.
- STEIN, S. and M. WYSESSION (2003). An introduction to seismology, earthquakes and Earth structure. Blackwell, Malden, USA, 498 pp.
- STOVER C. W. and J. L. COFFMAN (1993) Seismicity of the United States, 1568–1989 (Revised), U.S. Geological Survey Professional Paper 1527, U S Govt Print. Off., Washington.
- TAKEMURA, T. FURUMURA, and T. SAITO, (2009) *Distortion of the apparent S-wave radiation pattern in the high-frequency wavefield: Tottori-Ken Seibu, Japan, earthquake of 2000*. Geophys. J. Int. 178, 950–961.
- TAKENAKA, H.; MAMADA, Y.; FUTAMURE, H. (2003) *Near-source effect on radiation pattern of high-frequency S waves: strong SH-SV mixing observed from aftershocks of the 1997 Northwestern Kagoshima, Japan, earthquakes*. Phys. Earth Planet. Interiors, 137, 31–43.
- THATCHER, W. and HANKS, T. (1973), *Source parameters of Southern California earthquakes*. J. Geophys. Res. 78, 8547–8576.
- TRIFUNAC, M. D. (1993): Long period Fourier amplitude spectra of strong motion acceleration, Soil Dynam. and earthquake Eng., 12(6), 363–382.
- TRIFUNAC, M. D., and LEE V. W. (1989), *Preliminary empirical model for scaling Fourier amplitude spectra of strong ground acceleration in terms of earthquake magnitude, source to station distance and recording site conditions*, Earthq Eng Struct Mech, 18, 999–1016.
- TSAI, C. -C. P. (1997), *Ground motion modeling for seismic hazard analysis in the near-source regime: an asperity model*, Pure Appl Geophys, 149, 265–297 (0033-4553:97:020265-33).
- TSURUGI M., T. KAGAWA, and K. IRIKURA (2008). Study on high-cut frequency characteristics of ground motions for inland crustal earthquakes in Japan. Proc. 14 World Conference on Earthquake Engineering, October 12–17, Beijing, China
- WANG G., LI H., WANG D. and CHOW W.K. (2006) *Estimation Of Near-Fault Strong Ground Motions For Key Engineering Structures*. ISET J. Earthq. Technol., 43, 65–74.
- YOKOI, T. and K. IRIKURA (1991) *Meaning of source controlled  $f_{max}$  in the empirical Green's function technique based on  $\omega^2$ -scaling law*. Annuals, Disas. Prev. Res. Inst., Kyoto Univ., No. 34 B- 1, 177–189.
- YU, G., KHATTRI, K. N., ANDERSON, J. G., BRUNE, J. N., and ZENG, Y. (1995), Strong ground motion from the Uttarkashi, Himalaya, India, Earthquake: comparison of observations with synthetics using the composite source model, Bull Seism Soc Am, 85, 31–50.
- ZENG, Y., ANDERSON, J. G., and YU, G. (1994) *A composite source model for computing realistic synthetic strong ground motions*, Geophys Res Lett, 21, 725–728.

(Received January 31, 2011, revised August 31, 2011, accepted December 14, 2011)